EXO-NET®
TECHNICAL UPDATE
DECEMBER 2023

TABLE OF CONTENTS

EXO-NET is an affinity matrix, magnetic nanoparticle technology designed for isolating extracellular vesicles from biofluids and charactering their associated proteins, oligonucleotides and lipids using On-Bead Analysis or On-Bead Lysis.

1.   EXECUTIVE SUMMARY

Summary of the available data relating to the Company's EXO-NET® Pan-Exosome Product.

1.1   INTRODUCTION

The isolation of extracellular vesicles (EVs) from biofluids and characterization of their associated molecular cargo affords opportunity to identify tissue-specific biomarkers that may be useful in the earlier diagnosis of many diseases [1]. Although the compendium of disease-associated EV biomarkers identified continues to increase [2-10], there remains a paucity of EV diagnostics (EVDx) that have been translated into routine medical laboratory tests (for example, as a Laboratory Developed Test (LDT) implemented in a Clinical Laboratory Improvement Amendments (CLIA) laboratory) [11].   The challenge in implementing EVDx and LTDs has not been established and verifying the analytical performance specifications of EV-based tests (as defined by 42 CFR 493.1253) but the availability of simple, rapid, reproducible, high-throughput (i.e.,100s of samples per hour) EV isolation and downstream analysis.

To enable reproducible, high-throughput isolation of EVs from biofluids and the downstream analysis of RNA, protein and lipid biomarkers, INOVIQ has developed an affinity matrix magnetic nanoparticle technology (EXO-NET®) that can be customized for capturing and isolating subpopulations of EVs for on-particle analysis (e.g., Fourier Transformed InfraRed Spectroscopy) or on-particle lysis and for downstream analysis. The technology provides seamless transition from research and development (10s to 100s of samples) to CLIA laboratory workflows (100s to 1000s of samples).

EXO-NET Characteristics and Performance: EXO-NET is an affinity matrix magnetic nanoparticle technology product for the isolation of extracellular vesicles (EVs) from biofluids and the downstream analysis of associated proteins, oligonucleotides (mRNAs and microRNAs) and lipids.

The affinity matrix is built using 10 antibodies raised against transmembrane or cell surface proteins. The antibodies, two polyclonal (one goat, one sheep); one recombinant monoclonal rabbit; and seven mouse IgG monoclonals, are covalently linked to form an antibody matrix (~150 nm thick) around a paramagnetic bead with a diameter of 40-50 nm. EXO-NET is designed for *On-Bead* Analysis of affinity-captured particles, *e.g.,* FTIR or affinity ligand detection of vesicle surface epitopes, or On-*Bead Lysis* and downstream analysis of vesicle-associated analytes (Figure 1).

- EXO-NET captured EVs from pooled normal human plasma showed present of EV known protein markers CD63, CD81, CD9, Flotillin, TSG101 and EpCAM (Figure 9).
- EXO-NET isolates mRNA and mciroRNAs that are resistant to RNase A digestion (Figure 10-11) – data consistent with the capture of intact extracellular vesicles.
- EXO-NET plasma lysate contains archetypal EV mRNAs (Figure 10) and microRNAs (Figure 11).
- EXO-NET miRNAs and mRNAs yield, and recovery was higher compared with 4 other competitor products (Figure 12).
- EXO-NET isolates contain less contaminating high-abundance proteins than competitor products (Figure 13-14).
- High-throughput EXO-NET EV isolation establishment from cell conditioned medium (Figure 16).

2. INTRODUCTION

### 2.1 EXTRACELLULAR VESICLES

Extracellular vesicles (EVs) are a heterogeneous population of membrane-bound particles of around 30 nm up to a few micrometers in diameter. Most of these vesicles display a spherical, single bilayer morphology, however, vesicles with multiple membranes or with a tubular morphology also have been described [12]. Based on their biogenesis and physical properties, EVs are often classified as small EVs (including, exosomes) or large EVs (including, ectosomes or microvesicles, migrasomes and apoptotic bodies) and large oncosomes (Table 1). EVs are specifically packaged with signalling molecules, including lipids, proteins and nucleic acids, and are released via exocytosis or membrane budding into biofluid compartments. EVs regulate the activity of target cells, including translational activity, metabolism, growth and development. As such, EVs signalling represents an integral pathway mediating intercellular communication.

The term "exosome" has been used to refer to EVs of ~30-150 nm in diameter that are formed via the inward membrane budding of multivesicular bodies (MVBs). Upon fusion of MVBs with the plasma membrane, vesicles are released into the extracellular space and are subsequently referred to as exosomes. The content of such EVs may be regulated by Endosomal Sorting Complexes Required for Transport (ESCRT)-dependent and – independent mechanisms and further contribute to vesicle heterogeneity [13, 14]. The terms ectosome, microvesicle and microparticle have been used to characterize EVs that are formed through direct budding from the plasma membrane. Formation of microvesicles involves Ca^{2+} influx and contraction of cortical actin [15]. Finally, vesicular apoptotic bodies (up to a few microns) are formed when cells release membrane extrusions as part of the apoptotic process. They may contain nuclear and cytosolic fragments and even intact organelles. While apoptotic bodies are often regarded as unwanted contaminants of EV preparations, some argue that apoptotic bodies can also facilitate intercellular communication and may have potential as therapeutic modalities [16] (Figure 1).

TABLE 1: EV Subtypes				
EV SUB-TYPES	**SIZE**	**BIOGENESIS**	**CARGO**	**REFERENCES**
Exosomes	30-150 nm	Originate in the endosomal pathway in the multi-vesicular bodies (MVBs) and are released upon fusion of MVBs with the plasma membrane	proteins of the endosomal pathway and ESCRT complex (Alix, TSG101, HSP70) and members of tetraspanin family (CD62, CD9 and CD81)	[17-22]
Ectosomes (or microvesicles, microparticles)	50-1000 nm	Released by direct budding from the plasma membrane	Proteins Annexin A1, integrins, selectins, CD40	[23-26]
Migrasomes	500-3000 nm	Released from migrating cells, dependent onactin polymerization	protein TSPAN4	[27-29]
Apoptotic bodies	50-5000 nm	Released from apoptotic cells	protein Annexin V, lipid phosphatidyl serine	[24, 30, 31]
Large oncosomes	1000-10000 nm	Released from amoeboid cancer cells	protein cytokeratin 18	[32-34]
ARMMs (arrestin domain-containing protein 1 (ARRDC1)-mediated microvesicles)		Released via ARRDC1-driven outward budding of plasma membrane	Protein ARRDC1	[35, 36]

FIGURE 1: Overview of EVs Biogenesis
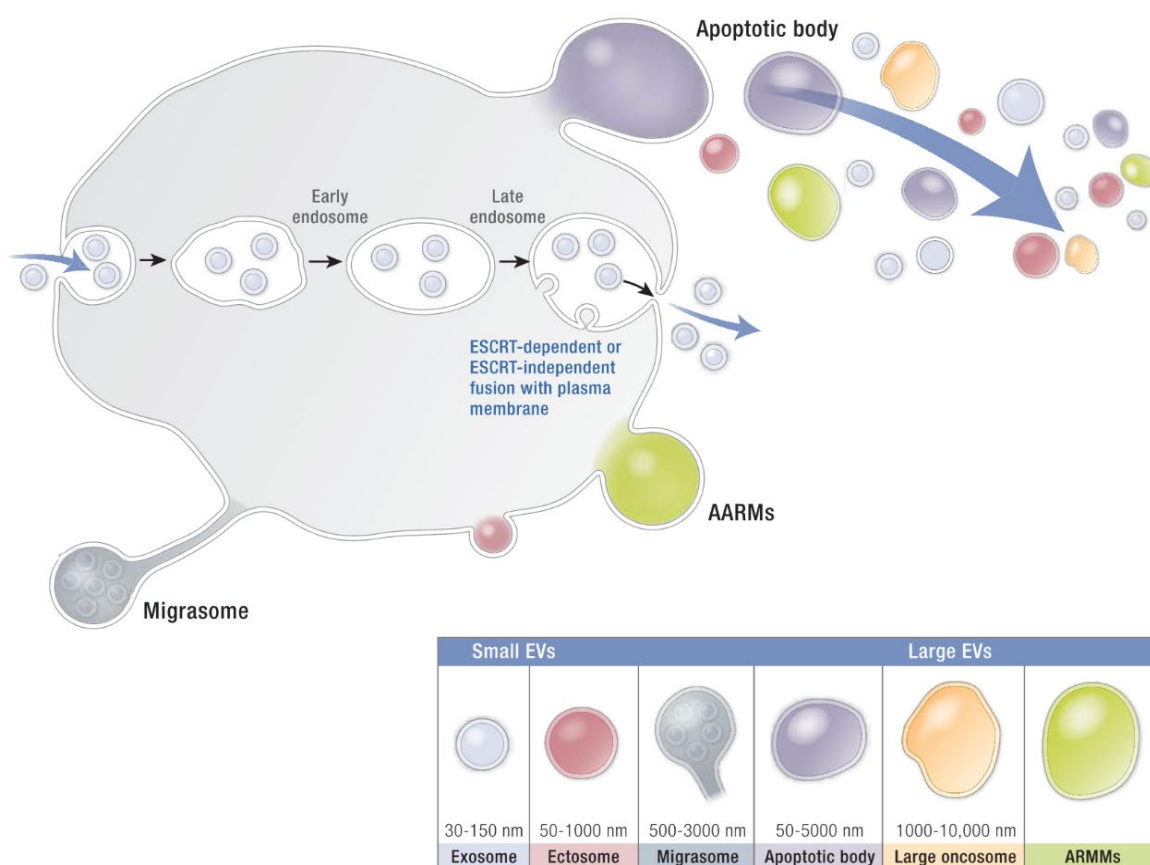
2.2   EV ISOLATION METHODS AND TECHNOLOGIES

Various methods and technologies (e.g., density gradient ultracentrifugation, size-exclusion chromatography, ultrafiltration) have been developed for isolating enriched subpopulations of EVs according to their dimension, whereas the fractionation of EV sub-classes of different cellular origin requires the use of affinity techniques. Current methods are limited by incompatibility with pathology laboratory workflows, long processing times and poor yield and purity. Immuno-capture-based approaches could represent an effective purification alternative to obtain homogeneous EV samples. Most studies of EV biomarkers are based on EVs that are isolated based on a single feature (e.g., density or size). Such approaches, however, lack specificity and poorly differentiate subpopulation of EVs. To enrich and interrogate subpopulations of EVs, the use of solid-phase, EV surface-specific ligands represent a feasible approach. Here, we present a novel bead-based immunoaffinity system that captures a highly enriched subpopulation of EV.
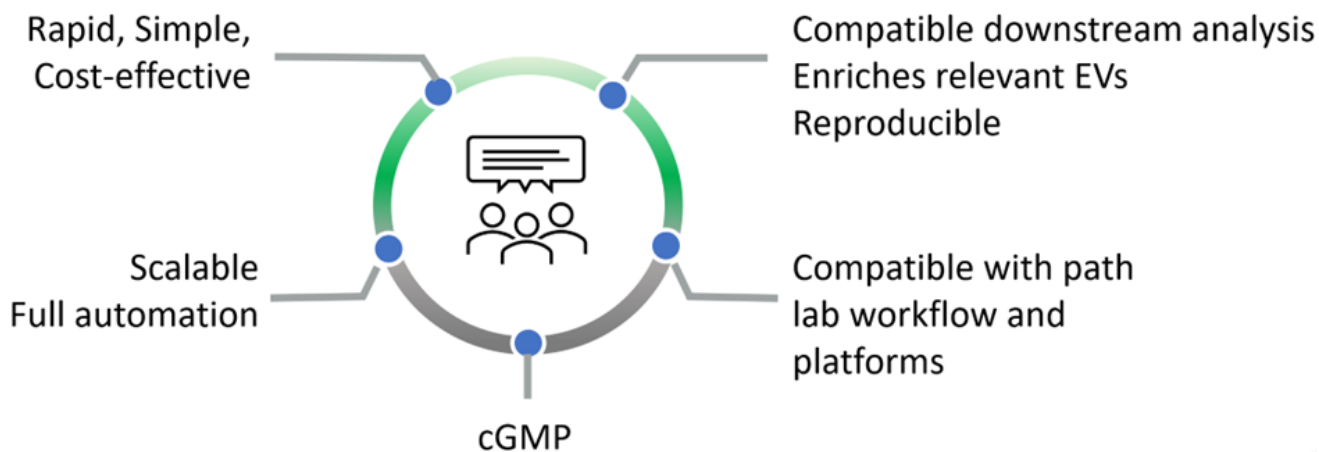
2.3   NET TECHNOLOGY

INOVIQ's "NET" products and pipeline are based on a proprietary solid-phase, 3-dimensional affinity matrix nanotechnology. The sequential construction of the 3D matrix increases the density and accessibility of ligand binding sites, thereby, increasing the efficiency. The NETs technology can be deployed on most solid-phase modalities, including, 96- and 384-well plates, polymer beads (suspension or column-based formats), magnetic beads and lateral flow devices. NET products are readily translatable formats for the development and implementation of fully automated applications for use in routine pathology service laboratories, (*e.g*., FACs, solution array and ELISA). NET products can be constructed to capture a wide range of biological targets, including viral particles, small and large extracellular vesicles, apoptotic bodies and cells. The capture ligands that may be incorporated into the NET include antibodies, high-affinity receptor proteins and aptamers.

2.4 DESIGN CONTROL

2.4.1 User Needs

User Needs – EV Isolation

Intended use -> A method for isolating and analyzing EV-subpopulations
[not based on features common to all extracellular particles]

Rapid, Simple, Cost-effective

Scalable
Full automation

cGMP

Compatible downstream analysis
Enriches relevant EVs
Reproducible

Compatible with path lab workflow and platforms

2.4.2 Design Inputs for EXO-NET

| INPUT	SPECIFICATION
Rapid	<2min avg per sample
High throughput	400 samples per day
Cost effective	Price competitive
Reproducible	Endpoint measure intra run CV <10% inter run CV <20%
Low sample volume	500 µg plasma 1 ml CCM
Total protein yield	< 10 µg/sample
Total RNA yield	< 3 µg/sample
Scalability	Manual & full automation
Compatibility	Isolates compatible with commercially available kits

INOVIQ

3. EXO-NET®

EXO-NET is one application of the *NETs* technology. EXO-NET is a magnetic bead-based immunoaffinity EV capture device, where a 3-dimensional antibody matrix is constructed on a carbon nanoparticle. The complement of antibodies attached to the bead has been designed to capture a wide range of EVs from different cell types (pan-EV capture). It is used to isolate EVs in solution and enable the downstream analysis of their associated cargo (including, proteins, oligonucleotides, lipids and metabolites). EXO-NET also can be tuned to preferentially isolate EVs from specific cell types.

EXO-NET is a scalable EV isolation solution for high throughput screening.
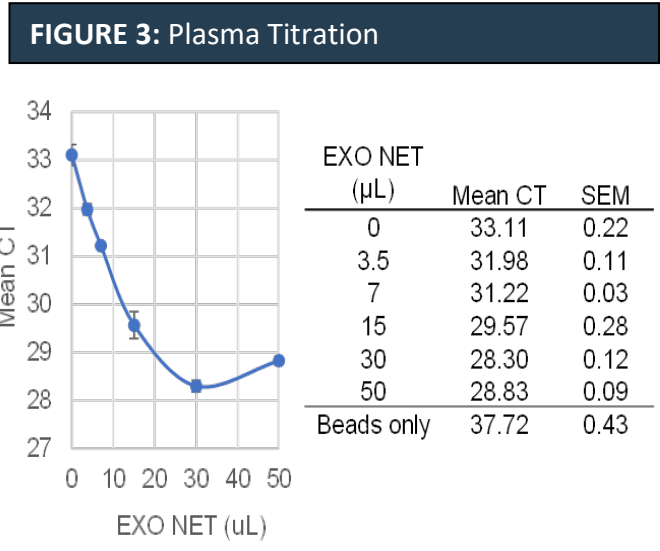
- Speed, purity and yield advantages
- Compatibility with downstream EV-associated analyte analyses
- Proprietary 3D affinity matrix for improved purity and yield
- Customizability and scalability for use with any biofluid sample
- Meeting an unmet need for the rapid, efficient, and scalable isolation of enriched exosomes.

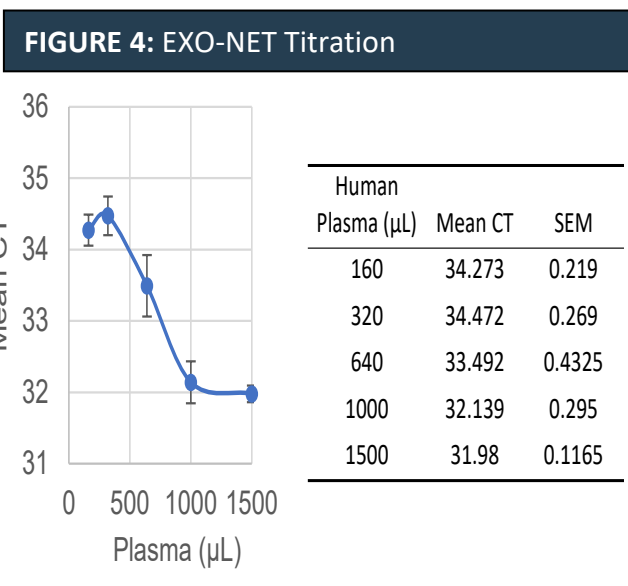**FIGURE 2:** EXO-NET Workflow for EV Capture
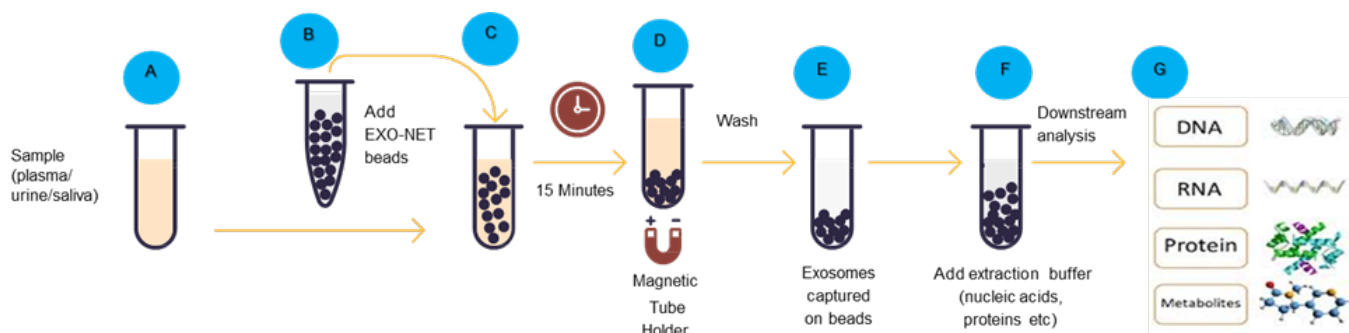
3.1 EXO-NET Titration

Plasma Titration: EXO-NET Titration studies are based on an input sample of human plasma and outcome measure of miR21 CT value. Experimental details: 0 (beads only) to 1500µL human plasma µL by adding DPBS. EXO-NET 15 µL EXO NET beads were added and incubated for 15 min @ RT. The beads were washed three times, each with 1 mL DPBS. After the final wash, the beads were suspended in 250 µL lysis buffer for RNA extraction. The RNA was eluted in 20 µL water and 12 µL was used to perform a reverse transcription reaction using the TaqMan miR21 probe. 4 µL of the cDNA was used for TaqMan miR21 qPCR reaction. Standard miR21 reactions were run using 1, 10, and 100 fM miR21. Data are presented as the mean CT values plotted (left panel) against the volume of plasma used and tabulated (R=right panel) (Figure 3).

FIGURE 3: Plasma Titration

EXO NET (µL)	Mean CT	SEM
0	33.11	0.22
3.5	31.98	0.11
7	31.22	0.03
15	29.57	0.28
30	28.30	0.12
50	28.83	0.09
Beads only	37.72	0.43

EXO-NET Titration: To determine the amount of EXO-NET needed to capture maximum amounts of exosomes from 500 µL human plasma, 3.7, 7, 15, 30, and 50 µL EXO NET beads (in triplicate, n = 3) were spread on top of the plasma samples by moving circularly partially submerged pipette tip while dispensing the beads. The tubes were inverted 5 to 10 times to form a homogenous plasma and EXO NET suspension. The tubes were incubated for 7.5 minutes at RT and a second mixing by inverting 5-10 times was done before incubating for an additional 7.5 min at RT. The beads were washed three times with 1 mL DPBS and mixed by inverting the tube 5 to 10 times. After the final wash, the beads were suspended in 250 µL lysis buffer for RNA extraction. The RNA was eluted in 20 µL RNAse free water and 12 µL of the eluted RNA was used to perform a reverse transcription reaction using TaqMan miR21 probe. For miR21 specific qPCR, 4 µL of the cDNA was used for TaqMan miR21 qPC reaction. Standard miR21 reaction was run using 1, 10, and 100 fM miR21 (Figure 4).

FIGURE 4: EXO-NET Titration

| Human Plasma (µL)	Mean CT	SEM
160	34.273	0.219
320	34.472	0.269
640	33.492	0.4325
1000	32.139	0.295
1500	31.98	0.1165

INOVIQ

3.2   CHARACTERIZATION OF EVS CAPTURED BY EXO-NET

EVs were isolated from human pooled plasma using EXO-NET. Nanoparticle tracking analysis (NTA, ZetaView) was used to analyse the particle size and number. The protein content of EXO-NET captured EVs was characterized by mass spectrometry and Western blotting. RT-qPCR was used to evaluate and quantify mRNA (GAPDH and OAZI) and microRNA cargo (miR-16, let-7a, miR-21) of isolated EVs from EXO-NET kit and other commercial kits.

3.3   NANOPARTICLE TRACKING ANALYSIS (ZETAVIEW)

FIGURE 5: EXO-NET beads nanoparticles analysis, as measured using ZetaView (Particle Metrix)

- The concentration and particle size profile of the EXO-NET beads are shown.

- The top graph shows the total particles in 20 aliquots of EXO-NET (10 µL each). The y-axis shows the calculated total particles, and the y-axis shows the sample number. The measurements were repeated twice with a %CV of 12 and an average of 1.76E+08 particles.

- The bottom graph shows the size distribution of EXO-NET beads. The median size is 73.47. The size range is from 5 nm to 385 nm. The y-axis shows the number of particles traced and the x-axis shows the particle size.
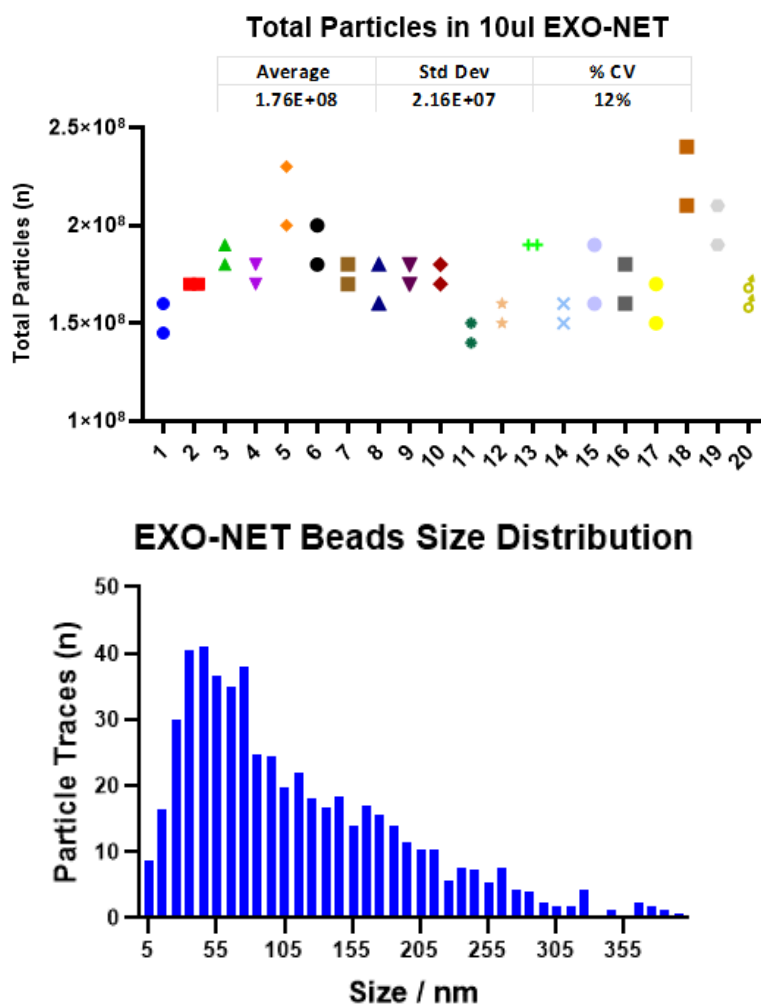
ZetaView analysis of EXO-NET beads showed that the average particle concentration in 10 µL of EXO-NET is around 1.76E+08 with a coefficient of variance of 12%. The size distribution of EXO-NET particles is also shown to be spread between 5nm to 385 nm with a median of 73.47 nm. Experimental Procedure: 20 separate aliquots of 10 µL of EXO-NET beads were measured using ZetaView nanoparticle analysis. Each measurement was repeated twice (Figure 5).

3.4 EXTRACELLULAR VESICLE PROTEIN RECOVERY

EXO-NET recovers a known extracellular vesicle protein (CD9)[37-41] from plasma.

Experimental Protocol: Pooled human plasma (200 µl) was incubated with increasing concentrations of EXO-NET (1.5, 3, 6, 15, and 30 µl) for 15 min at room temperature. Plasma-loaded EXO-NET was magnetically sedimented and washed 3 times in phosphate buffered saline (PBS, pH 7.4) and then resuspended in 0.001% (v/v) Tween 20 and boiled to release EXO-NET associated proteins. The supernatant fluid was subjected to SDS PAGE gel electrophoresis and stained with Coomassie Blue for total protein (Figure 6) or subjected to Western blot analysis to identify and semi-quantify immunoreactive CD9 (using the antibody ab92726 at a 1:1000 dilution). An EXO-NET dose-dependent increase in a signal at 24 kDa related to CD9 was observed (Figure 7). A quantitative analysis of 10 plasma samples is presented in Figure 8. Furthermore, EXO-NET derived EVs were characterized using EVs known protein markers (CD63, CD81, CD9, Flotillin, TSG101 and EpCAM). EXO-NET derived EVs from pooled human plasma showed presence of all these proteins (Figure 9).

FIGURE 6: Commassie-stained gel of plasma (200Ul) protein isolated by increasing volumes of EXO-NET (3, 6, and 15Ul). The eluted proteins from EXO-NET were separated using SDS-PAGE.
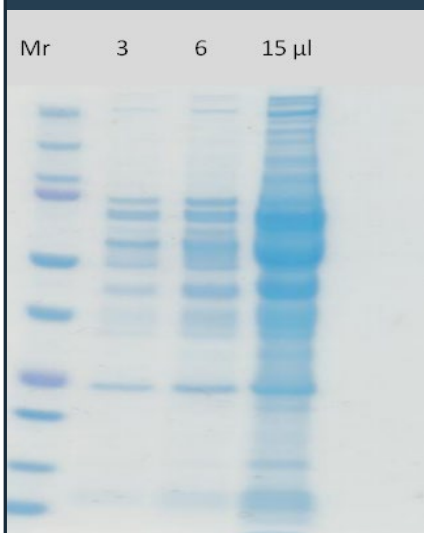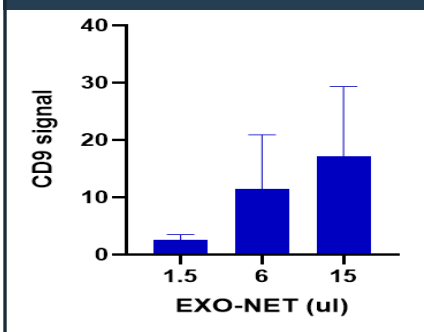
FIGURE 7: CD9 Western blot of an EXO-NET isolate of human plasma (panel A). Exosomes were isolated from 200 µl of human plasma using increasing concentrations of EXO -NET (1.5 –30 µl). 30 µL of EXO-NET without plasma was used as control. [SEC= a size exclusion comparator]. A linear relationship was observed between EXO-NET volume and CD9 signal (panel B).
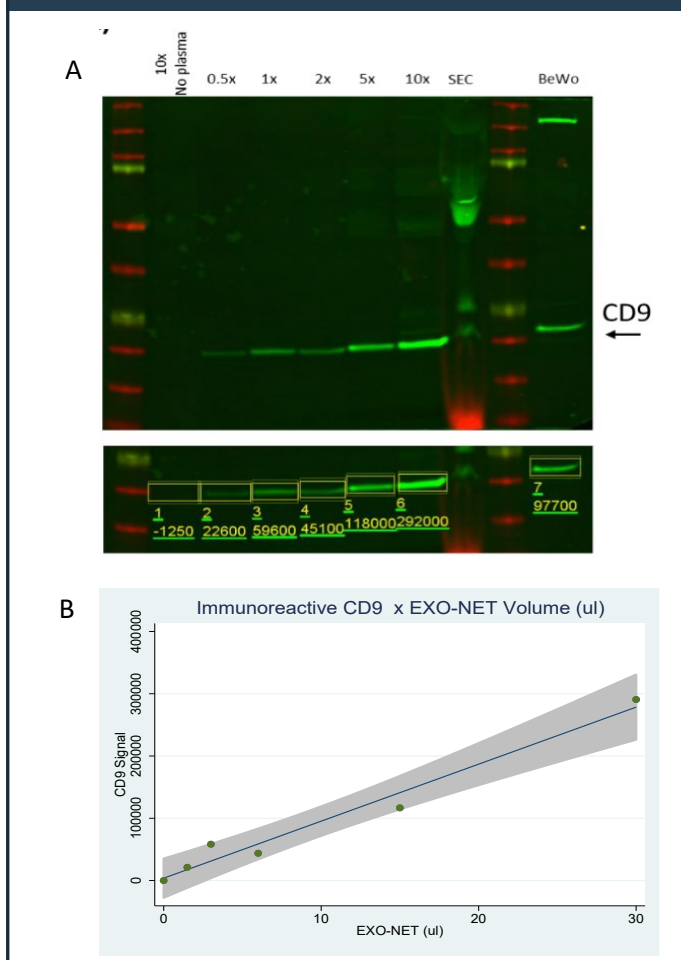

FIGURE 8: Quantitative analysis of immune-reactive CD9 present in EXO-NET (1.5, 3, 15 µl) isolated of human plasma (n=10).

FIGURE 9: Western blot analysis of EXO-NET captured EVs from normal human plasma

Classical extracellular vesicle markers were evaluated in EV isolated from 200-500 µl of human plasma using EXO-NET (15-30 µl). For TSG101, CD81 and CD63 detection EVs were isolated from 500 µL of plasma and 30 µL of EXO-NET. For CD9, Flotillin-1 and EpCAM, EVs were isolated from 200 µL of plasma and 15 µL of EXO-NET.

All the primary antibodies were diluted in 1:500 using wet-chamber method and incubated with secondary rabbit antibody at 1:2000 dilution. The markers selected for the characterization follow the MISEV 2018 guidelines. CD63 and CD81, tetraspanins from group 1a: non-tissue specific. CD9, tetraspanin from group 1b: cell/tissue specific. TSG101, protein from group 2a: member of ESCRT machinery. Flotillin-1, also from group 2a as accessory protein. EpCAM, protein in group 1b as derived from epithelial cells.

CD63 (25, 30-60 kDa) CD81 (22 kDa) CD9 (22, 24, 35 kDa) TSG101 (50 kDa) Flotillin-1 (49 kDa) EpCAM (40 kDa)
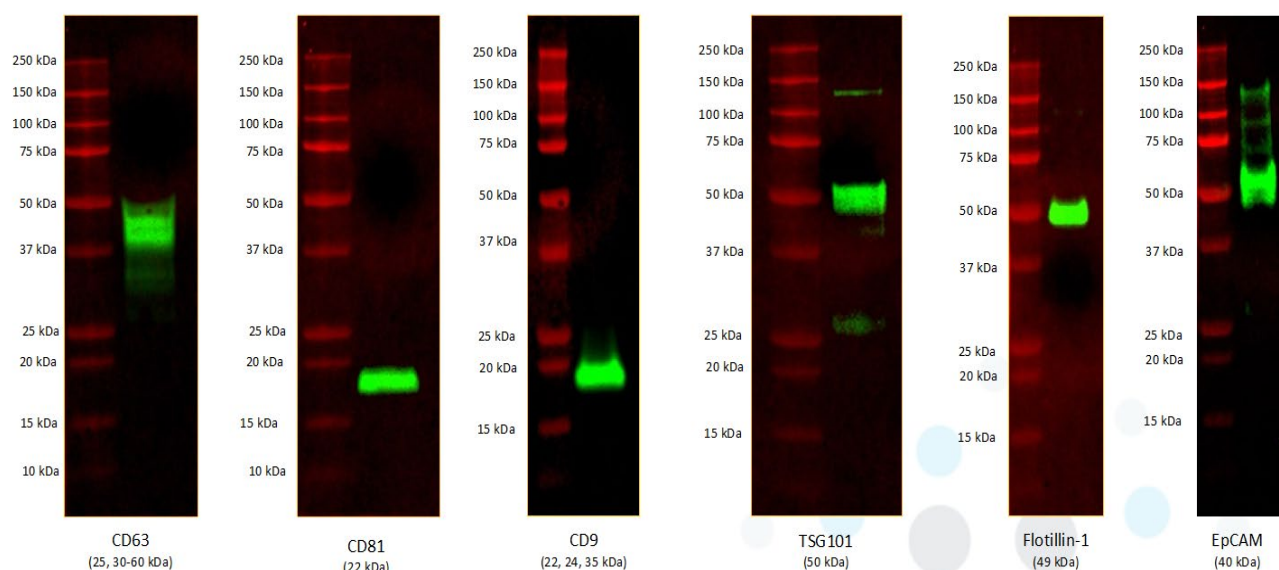
3.4 EXTRACELLULAR VESICLE RNA RECOVERY

To demonstrate that EVs isolated using EXO-NET are intact, and that the RNA associated with EXO-NET is contained within vesicles, plasma-loaded EXO-NET was treated with RNase A to degrade all accessible RNA (*i.e.,* RNA not encapsulated and protected within a vesicle). The samples were then subjected to RNA extraction and miRNA quantification.

Experimental Protocol: After capturing plasma EVs on EXO-NET beads, they were incubated in PBS, RNase A (6.2 µg/mL PBS), Triton X-100 (0.1% v/v, to disrupt the exosome membrane) or both RNase A and Triton X-100 for 30 min. As an additional negative control, exosomes were directly lysed to extract total RNA. If RNA transcripts are contained within EVs then RNAse treatment should not affect the total amount of RNA quantified by RT qPCR. The corollary is that a decrease in total RNA (*i.e.,* an increased CT value) post-RNAse treatment is indicative that EXO-NET associated RNA is not protected within vesicle and was degraded. Samples were assayed by RT-qPCR for mRNAs (GAPDH and RPLP0 and miRNAs miR-16, let-7a, and miR-21 (Figure 10 and Figure 11).

FIGURE 10: EXO-NET-associated mRNA is resistant to RNase A digestion. Metrix)

Mean CT values for GAPDH and RPLP0 mRNA captured from plasma. Plasma-loaded EXO-NET was treated with RNase A (6.25 µg/mL) or RNase A (6.25 µg/mL) with 0.1% Triton X-100. Mean CT values were not affected by RNase treatment alone, but degradation was observed following membrane disruption (detergent treatment).

FIGURE 11: EXO-NET captures RNase-resistant, detergent-labile miRNA

EXO-NET-associated miRNA is resistant to RNase A digestion. Mean CT values for let7a, miR16 and miR21 miRNAs. Plasma-loaded EXO-NET was treated with RNase A (6.25 µg/mL), Triton X-100 or a mix of RNase A (6.25 µg/mL) with 0.1% Triton X-100. Mean CT values were not affected by RNase treatment alone, but degradation was observed f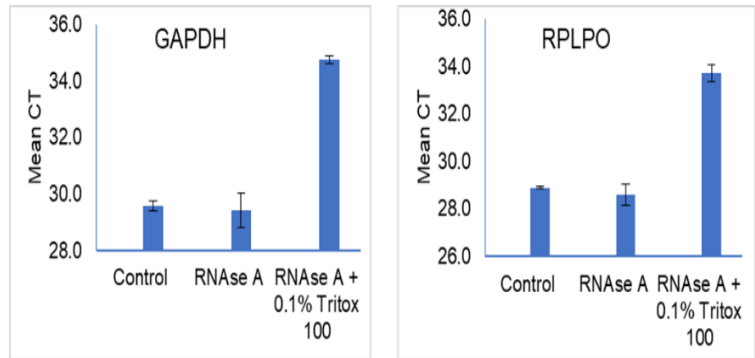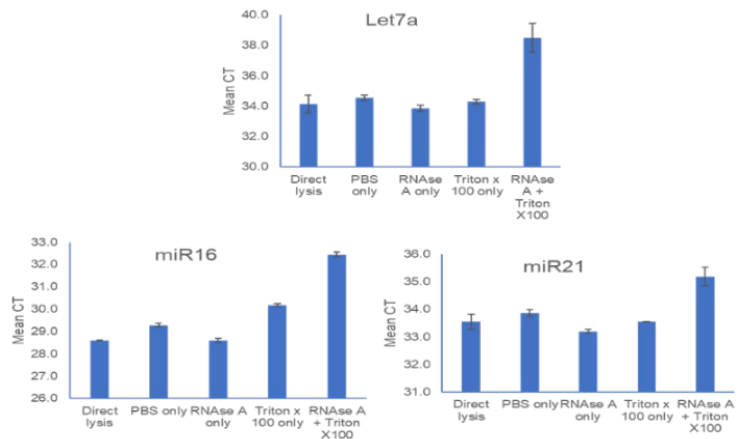ollowing membrane disruption (detergent treatment). These data are consistent with the encapsulation of miRNA with particles captured by EXO-NET.

INOVIQ

4. EXO-NET COMPETITOR COMPARISON

Several different methods have been used over the past decade to isolate particulate fractions (i.e., EVs) from biological fluids, including differential and buoyant density centrifugation, precipitation, filtration, size exclusion chromatography and solid phase immunoaffinity capture. A recent statement prepared for the Endocrine Society [1] reviewed the key performance characteristics of these approaches. Their findings are summarised in Table 2.

The key features for EV isolation are the length of operation time (Time), cost of the equipment and consumables (Cost), the ease of scaling the technique to process large volumes of fluids (Scalability), the percentage of EVs in fluids that could be extracted (Recovery) and the ratio of EVs extracted relative to total protein (Specificity). Using these criteria, the best performing method was immunoaffinity magnetic bead capture. EXO-NET is an immunoaffinity magnetic bead capture system that scores highly in all key criteria, in addition, it has been fully automated for high-through put sample processing (384 well format plates) by one of INOVIQ's academic collaborators.

TABLE 2: Comparison of the key features in commonly used EV enrichment techniques					
EV Enrichment Techniques	**Time**	**Cost**	**Scalability**	**Recovery**	**Specificity**
Polyethylene glycol precipitation	+++	++++	++++	++++	+
Size exclusion chromatography	+	+	+	+	+++
High MW centrifugal filters	++++	+++	++++	+++	++
Differential ultracentrifugation	+	++	+	+	++
Tangential flow filtration	+++	++	++++	+++	+++
Affinity chromatography	++	+	++	++	++++
Immuno-magnetic bead capture*	++++	+++	+++++	+++	++++

+ denotes the desirability of the feature | ++++: most desirable and +: least desirable

4.1 RNA RECOVERY COMPARISON

To further evidence the performance of EXO-NET, it was benchmarked against 4 other EV isolation products on the market which are listed below. EVs were isolated from pooled plasma samples using these four different methods, according to manufacturer's instruction. The outcome measure of performance was recovery of mRNA (GAPDH, OAZI, RPLP0and ZERF2) and miRNA (miR-16, let-7a and miR-21), as determined by RT qPCR. The data are presented in Figure 12.

1. Qiagen exoRNeasy (QIAGEN GmbH, Hilden, Germany)
2. Norgen Plasma/Serum Exosome Purification Kit (Norgen Biotek Corp., Ontario, Canada).
3. Thermo Fisher Invitrogen Total Exosome Isolation Kit (Thermo Fisher, Waltham, MA).
4. SBI ExoQuick Plasma prep and Exosome precipitation kit (System Biosciences, LLC., Palo Alto, CA).

FIGURE 12: Overview of miRNAs (top panel) and mRNAs (lower panel) yield and recovery using EXO-NET and 4 other competitor products were assayed by RT-qPCR for miRNAs miR-16, let-7a and miR-21 and mRNA for GAPDH, OAZ1, RPLPO and ZERF2. *mRNA level was below the limit of detection. EXONET results in equivalent or higher recovery of EV RNA compared to 4 commercial EV isolation kits as indicated by a lower CT value.


EXO-NET comparison to 4 commerical kits - miRNA

EXO-NET comparison to 4 commerical kits - mRNA

4.2 MASS SPECTROMETRY ANALYSIS COMPARISON

4.2.1 Serum protein contamination comparison by mass spec

The superior performance of EXO-NET to minimize contamination of EVs by plasma proteins was demonstrated by quantifying serum albumin present in the EV preparation of three competitor products and comparing it to EXO-NET isolated EVs.

Experimental Protocol: EVs were isolated from human plasma according to manufacturers' instructions. Proteins present in the EV isolates were then analysed using LC MS/MS. Contamination of the preparations by the co-isolation of serum albumin was expressed as the sum of the intensity of albumin peptide fragments identified (Figure 13).


FIGURE 13: Mass spec analysis of contaminant albumin intensity between EXO-NET captured EVs vs another magnetic bead-based method.

Albumin peptide intensity of EV preparations, measured by mass spectrometry. The albumin peptide intensity in competitor EV preparations was 2 to 3-fold greater than that observed in EXO-NET EV preparations. EXO-NET reduces the contamination of EV preparations with serum proteins that may confound downstream analysis.
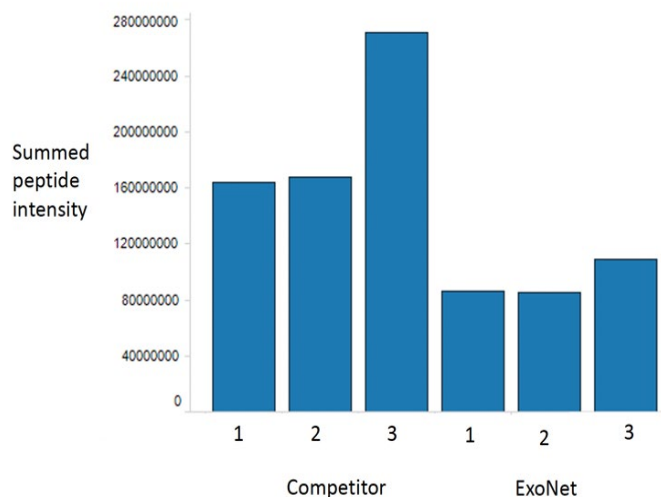
4.3 EV PROTEIN RECOVERY BY MASS SPEC

The superior performance of EXO-NET to isolate known EV-associated proteins was assessed in the same experiment described above. The total peptide intensity of proteins that have been reported to be routinely associated with EVs was determined for competitor products and EXO-NET (Figure 14).

FIGURE 14: Mass spec analysis of peptide intensity of EVs associated proteins between EXO-NET captured EVs vs another magnetic bead-based method.

The EV peptide intensity in competitor EV preparations was 6 to 10-fold less than that observed in EXO-NET EV preparations. These data are consistent with EXO-NET delivering a higher enriched preparation of EVs than the competitor products.

INOVIQ
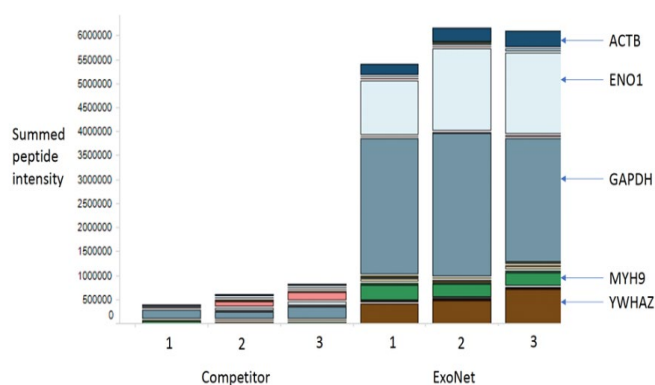
4.4 PROTEIN RECOVERY COMPARISON BY WESTERN BLOTTING

To compare the EV capture efficiency, purity of captured EVs and released product for downstream analysis, we compared protein profiles of EVs captured by EXO-NET along with commercial bead- and precipitation-based, size exclusion column-based EV capture tools. EVs from 200 µL of breast cancer plasma were captured using EXO-NET and two comparable bead-based EV capture kits, one EV precipitation-based kit and one size exclusion column-based kit. The captured/precipitated EVs were lysed using RIPA protein lysis buffer and equivalent amount of protein was analysed using PAGE gel and Oriole fluorescent gel staining solution. The protein profile showed that EXO-NET released protein is distinct from total plasma protein profile and is relatively cleaner compared to the other EV capture kits.

Experimental Protocol: Breast cancer plasma was centrifuged at 10,000 x g for 5 minutes and aliquoted to 200 µL per 1.5 mL microfuge tubes. 15 µL EXO-NET beads were added to one batch of three tubes and incubated for 15 minutes at RT. The EXO-NET and captured EVs were separated by incubating the tubes on a magnetic rack. The captured EVs were further washed three times using 1 mL dPBS. The EVs from rest of the breast cancer plasma aliquots were isolated using two comparable bead-based EV capture kits (Exosome Isolation Kit Pan, human- Milteni and Plasma/Serum Exosome Purification and RNA Isolation Mini Kit, Norgen), one precipitation-based EV capture kits (ExoQuick Plasma prep and Exosome precipitation kit, System Biosciences) and one size exclusion column-based EV isolation kit (IZON column, IZON). The captured EVs were lysed using RIPA protein lysis buffer and equivalent amount of protein was loaded on 16% tris Glycine PAGE gel. The proteins were visualized by staining with Oriole fluorescent gel staining solution (Figure 15).

> **FIGURE 15:** (A) SDS-PAGE profile of EXO-NET and 4 other commercial exosome isolation kits shows that EXO-NET released protein is distinct from total plasma protein profile and is relatively cleaner compared to the other EV capture kits. (B) Western blot analysis of EV captured by EXO-NET and 3 other competitor kits. EV were isolated from human pooled plasma and were analysed for the presence of EV protein. EXO-NET successfully enriched for abundance of EV protein (Flotillin-1) relative to competitor kits. EXO-NET captured EVs were absent of EV contaminating protein (ApoB) compared to other kits which had high abundancy of EV contaminating protein.

INOVIQ
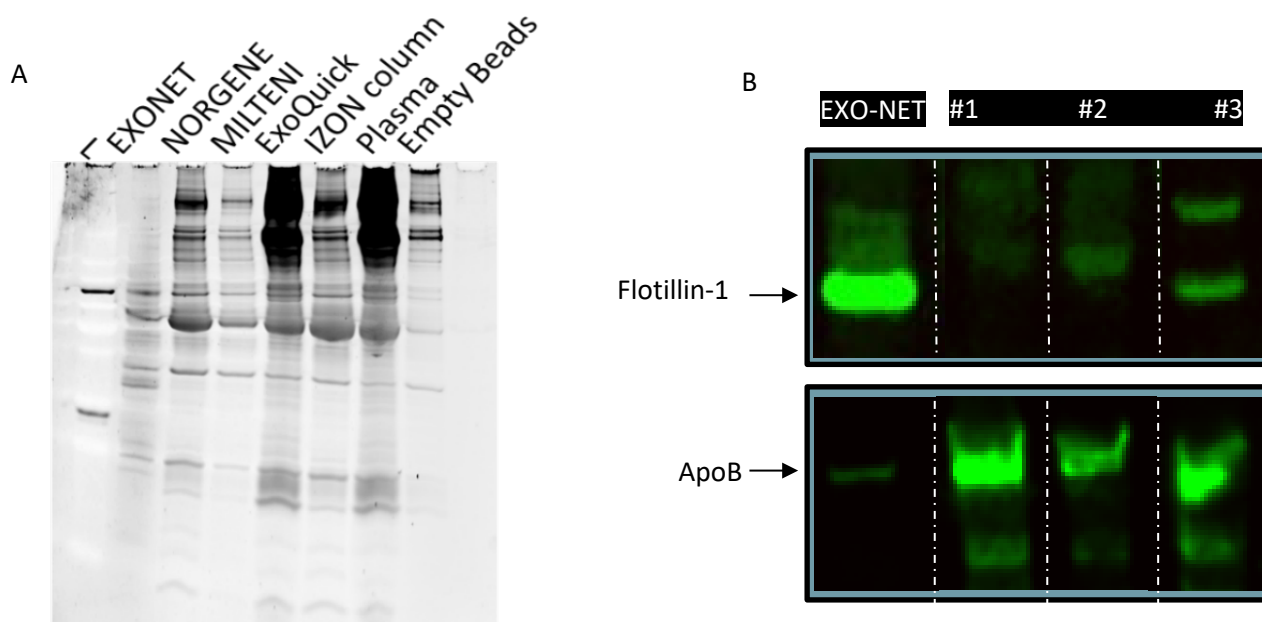
5. APPLICATION EXAMPLES

5.1 EXO-NET CAPTURED EVS FROM CELL CONDITIONED MEDIUM

Next was to demonstrate versatility of EXO-NET for isolating EVs from cell-conditioned medium (CCM). EVs were isolated from 1mL of CCM from MCF-7 cell line (human breast cancer) both manually (n=10) and on high-throughput automated system called KingFisher Apex. Captured EVs were assessed by RT-PCR and Western blot for miRNA (miR21 and miR186) and protein markers (CD9) respectively (Figure 16). RT-PCR analysis showed that EXO-NET EV derived miRNA (miR-21 and miR-186) yield and recovery were similar between automated and manual isolation. Western blot analysis demonstrated that EXO-NET captured EVs from both automated and manual isolation were positive for CD9 confirming successful isolation of CCM derived EVs. The use of EXO-NET for isolating EVs from CCM and the downstream analysis of EV-associated proteins, nucleic acids and lipids can be achieved using as little as 1mL CCM and does not require CCM to be concentrated prior to EV isolation. Nor does it require sample processing post-EV fractionation (e.g., concentration using Amicon filters). Conservatively, using EXO-NET to isolate and characterized CCM-EV reduces total isolation time from 8 h per batch to 60 min.

> **FIGURE 16: EXO-NET captured EVs characterisation from CCM (automated isolation vs manual).** EVs were isolated from 1mL of pooled cell conditioned medium (MCF-7 cell line) using EXO-NET (30µL) manually or on the KingFisher Apex instrument (n=10/each group). (A) RT-PCR analysis of EXO-NET captured EVs from automated system vs manual isolation. Total RNA was extracted from captured EVs by manual ReliaPrep RNA Cell Miniprep System (Promega) or automated Maxwell RSC miRNA Plasma and Serum kit (Promega). The yield and recovery of microRNAs (miR21 and miR186) were similar or even better (lower CV) than manual EV isolation. (B) Western blot analysis of EXO-NET captured EVs from CCM. Isolated EVs were lysed in 30ul of 1% SDS and equal amount of protein (6-9 µg of protein/ lane) were loaded to detect the expression of CD9.Western blot analysis showed EXO-NET-isolated EVs from both automated and manual isolation were positive for CD9.
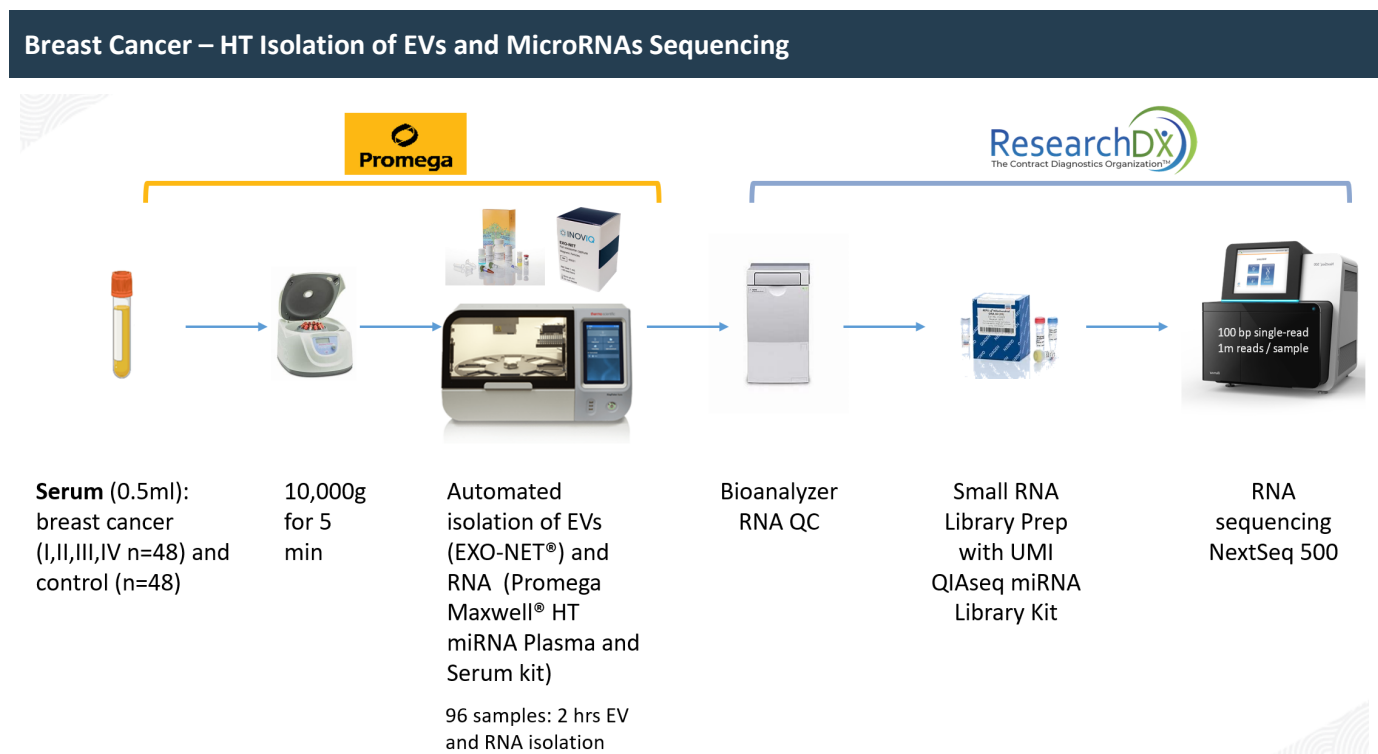
INOVIQ
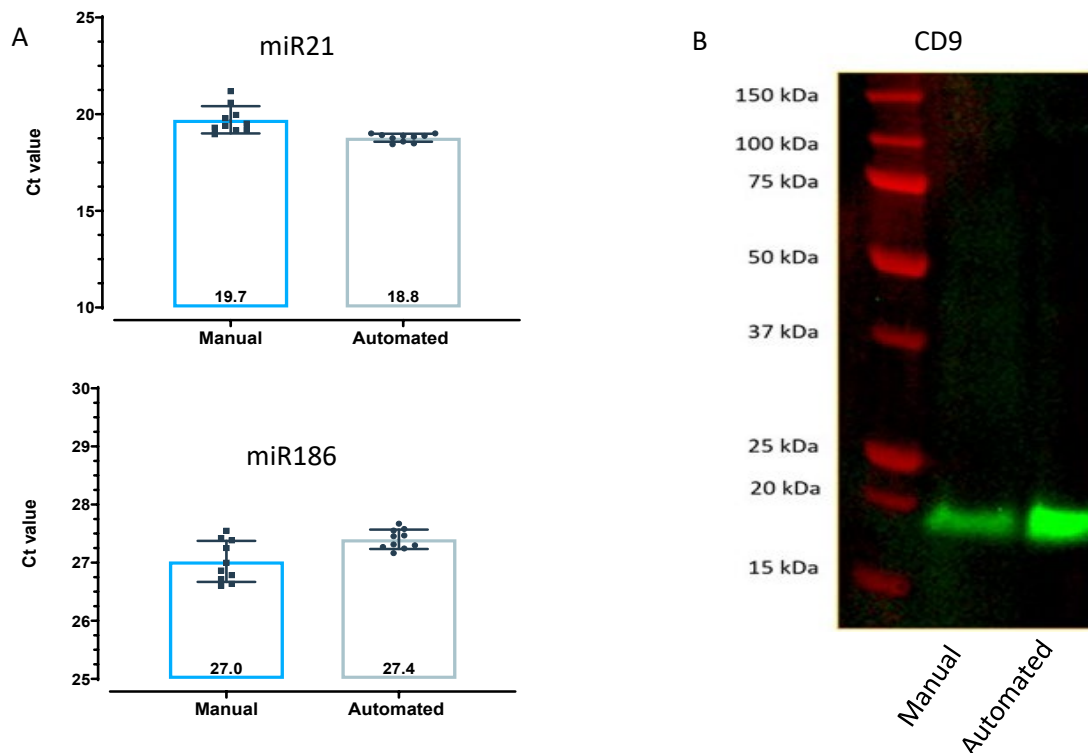
5.2 HIGH-THROUGHPUT MIRNASEQ ANALYSIS OF EXO-NET ISOLATED SERUM EVS

5.2.1 Breast Cancer

Aim: Identify differentially expressed miRNAs in a subpopulation of EVs isolated from serum samples obtain from normal healthy women and women diagnosed with breast cancer.

Intended Use: For research of treatment response monitoring, disease recurrence.

Project Plan:

Breast Cancer – HT Isolation of EVs and MicroRNAs Sequencing

Serum (0.5ml): breast cancer (I,II,III,IV n=48) and control (n=48)

10,000g for 5 min

Automated isolation of EVs (EXO-NET®) and RNA (Promega Maxwell® HT miRNA Plasma and Serum kit)

96 samples: 2 hrs EV and RNA isolation

Bioanalyzer RNA QC

Small RNA Library Prep with UMI QIAseq miRNA Library Kit

RNA sequencing NextSeq 500

Results:

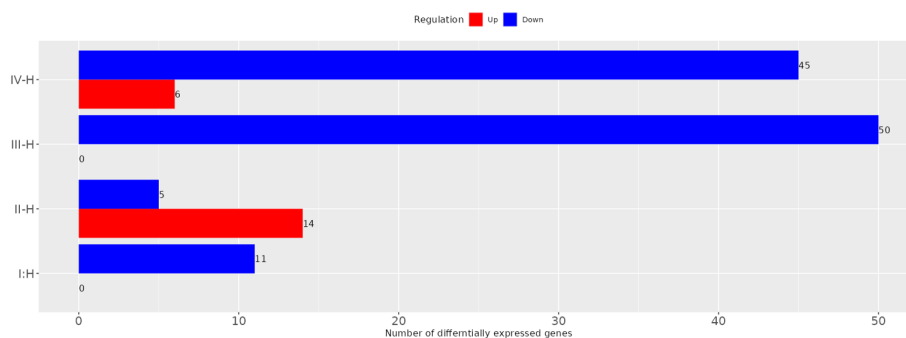| Differentially Expressed Serum EV miRNA |
|---|

Data
Species:
Number of samples: 96
Number of genes converted and filtered: 2652
5 sample groups detected.
Input file type: RNA-seq read count file

Pre-processing and exploratory data analysis settings:
Min. counts: minCounts= 10
Min. counts samples: NminSamples= 1
Counts data transformation method: Started log: log2(x+c)
Pseudo count: c= 10
Method for differential expression: CountsDEGMethod= 3 (DESeq2)
number of genes in heatmap: nGenes= 1000
number of genes in k-means clustering: nGenesKNN= 2000
number of clusters in k-means clustering: nClusters= 4
Promoter analysis for k-means clustering: radioPromoterKmeans= 300 bp

Differential expression settings:
FDR cutoff: limmaPval= 0.1
Fold-change cutoff: limmaFC= 2
Promoter analysis for DEGs: radio.promoter= 600 bp

Pathway analysis settings:
Pathway analysis methods: pathwayMethod= NA
FDR cutoff: pathwayPvalCutoff= 0.2
Min size for gene set: minSetSize= 5
Max size for gene set: maxSetSize= 2000

PREDA settings:
FDR cutoff: RegionsPvalCutoff= 0.01
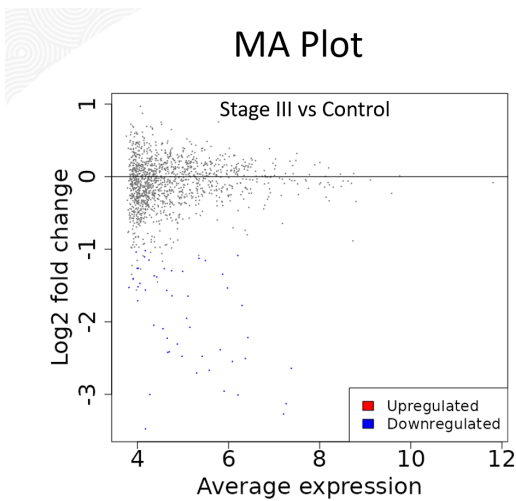FDR cutoff: StatisticCutoff= 0.5

Comparisons	Up	Down
IV-H	6	45
III-H	0	50
II-H	14	5
I:H	0	11

Differentially Expressed Serum EV miRNA

Stage 3&4 vs normal

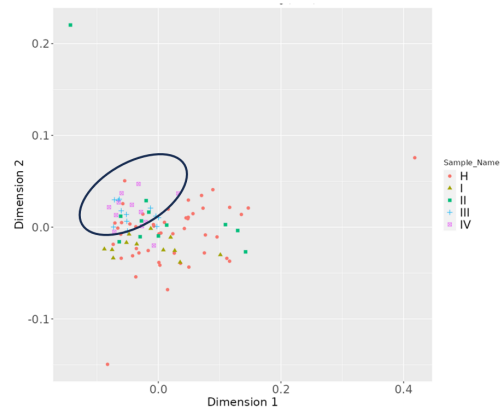

Top 10 negative and 10 positive miRs
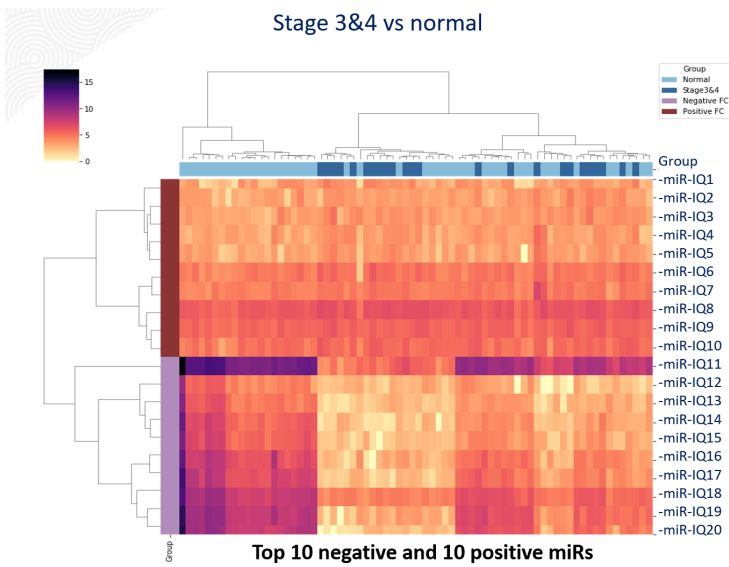
INOVIQ EXO-NET® **+ Promega** Maxwell® HT miRNA Plasma and Serum identifies differentially expressed breast EV-associated miRNA from 500 µl serum
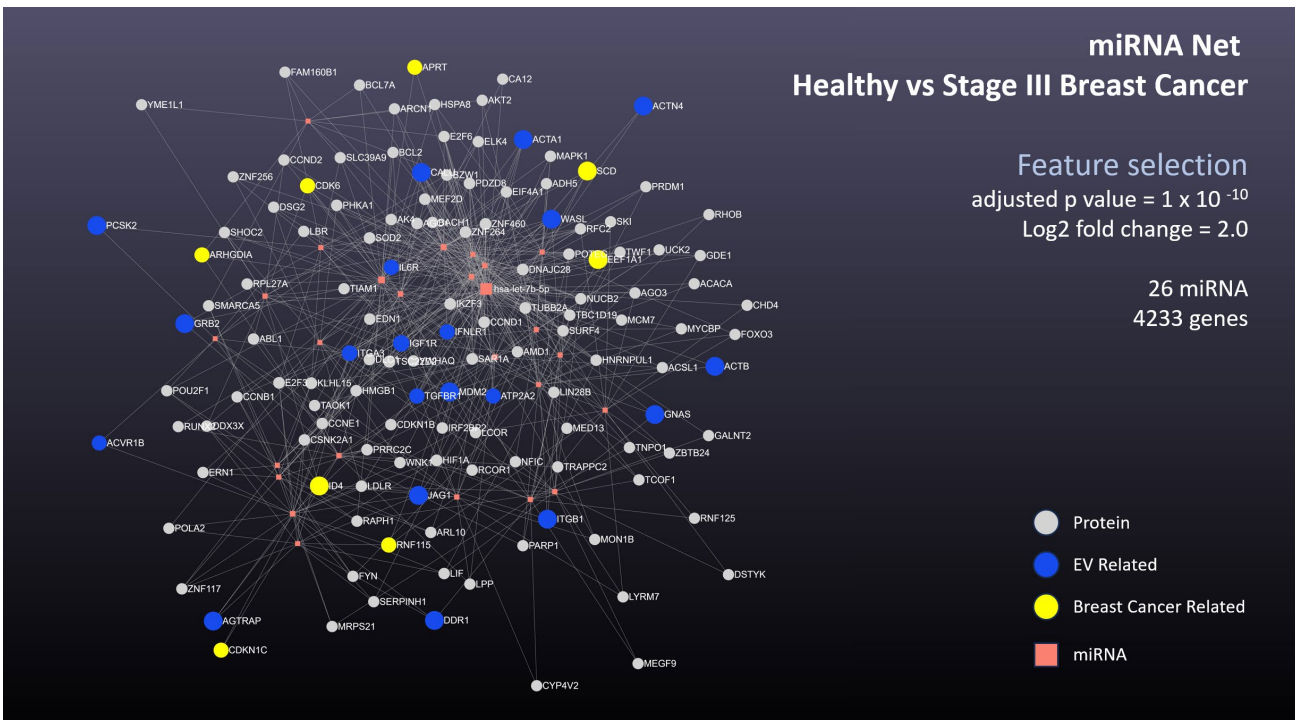
Data Modelling

MA Plot

Multidimensional scaling

INOVIQ EXO-NET® **+ Promega** Maxwell® HT miRNA Plasma and Serum Kit enables EV cargo analysis

INOVIQ

miRNA Net
Healthy vs Stage III Breast Cancer

Feature selection
adjusted p value = 1×10^{-10}
Log2 fold change = 2.0

26 miRNA
4233 genes

Protein
EV Related
Breast Cancer Related
miRNA

Outcome: miRNA obtained using EXO-NET® and Maxwell® HT miRNA Plasma and Serum kit on a high-throughput, fully automated platform was fit-for-purpose for miRNASeq

Identifying significantly differentially expressed miRNAs (log2 =2, p <0.01) from a subpopulation of serum EVs obtain from normal healthy women and women diagnosed with breast cancer.

Data modelling identified molecular pathways associated with breast cancer and EV compartments.

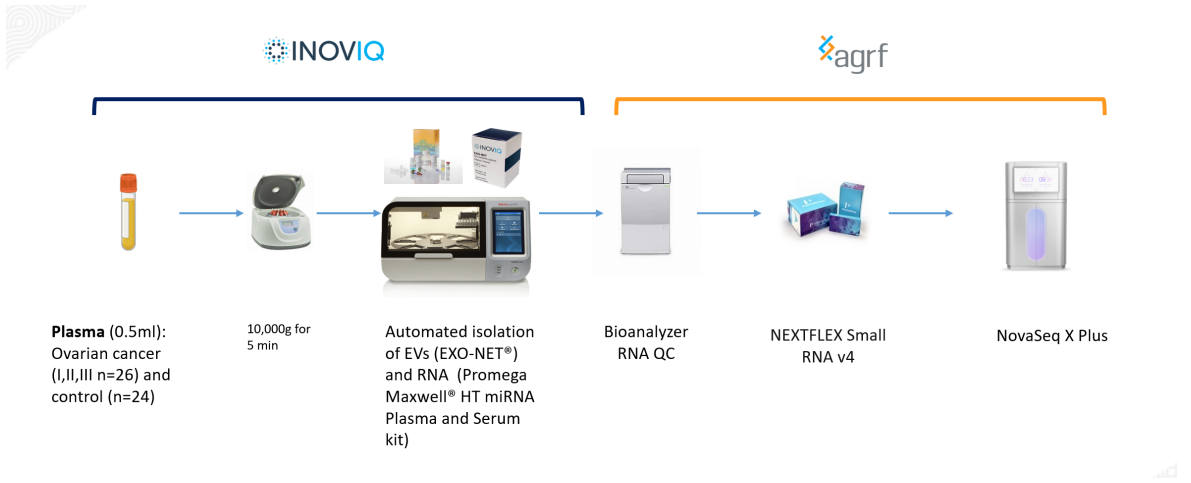### 5.3 HIGH-THROUGHPUT MIRNASEQ ANALYSIS OF EXO-NET ISOLATED PLASMA EVS

5.3.1 Ovarian Cancer

Aim: Identify differentially expressed exosomal miRNAs in a subpopulation of EVs isolated from plasma samples obtain from normal healthy women and women diagnosed with ovarian cancer.

For Research of: treatment response monitoring, disease recurrence.

Project Plan:

Ovarian Cancer – High Throughput Isolation of EVs and miR Sequencing

Plasma (0.5ml): Ovarian cancer (I,II,III n=26) and control (n=24)

10,000g for 5 min

Automated isolation of EVs (EXO-NET®) and RNA (Promega Maxwell® HT miRNA Plasma and Serum kit)

Bioanalyzer RNA QC

NEXTFLEX Small RNA v4

NovaSeq X Plus

INOVIQ

Results:

Differentially Expressed Plasma EV miRNA
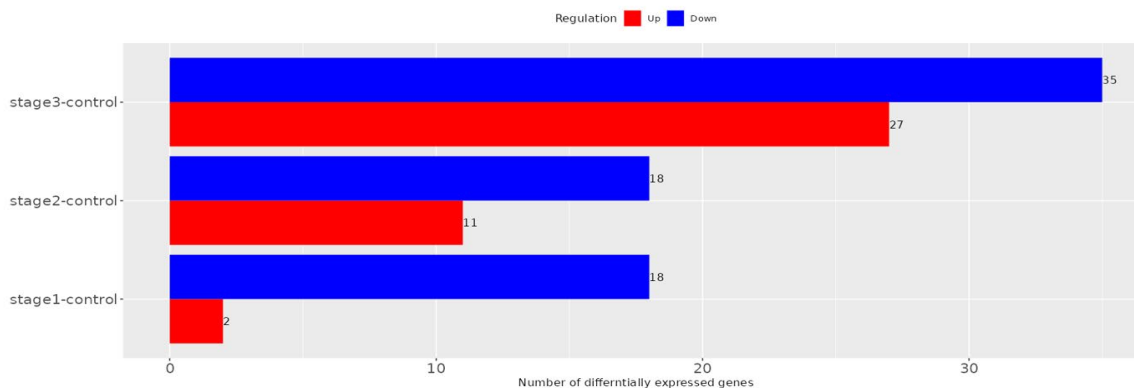
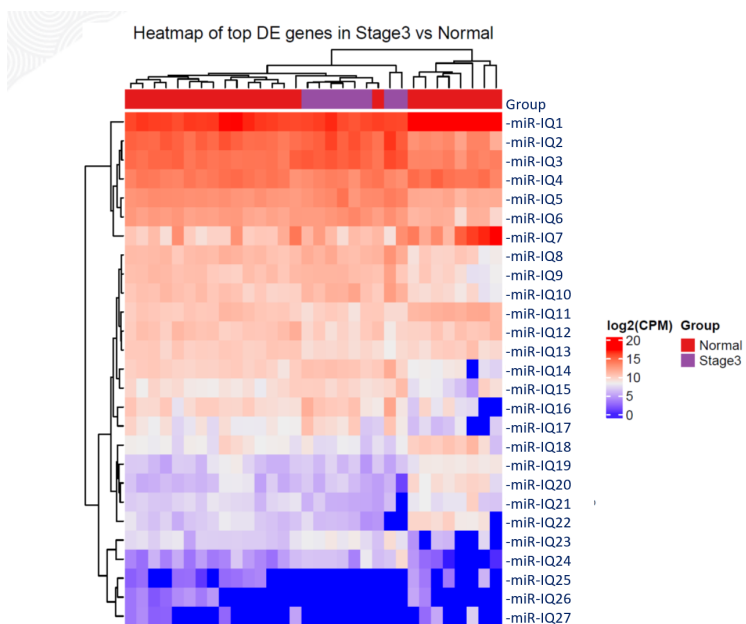| Comparisons	Up	Down
stage3-control	27	35
stage2-control	11	18
stage1-control	2	18

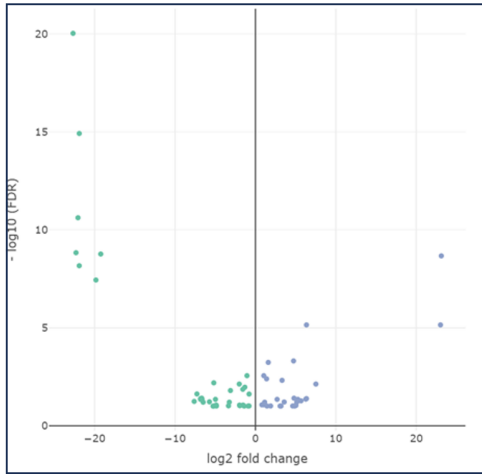## Top Differentially Expressed Genes in Stage 3 vs Normal

Heatmap of top DE genes in Stage3 vs Normal

INOVIQ EXO-NET® **+ Promega** Maxwell® HT miRNA Plasma and Serum identifies 27 significant differentially expressed breast EV-associated miRNA from 500 µl plasma

Data Modelling

Volcano Plot

Multidimensional scaling

case vs control
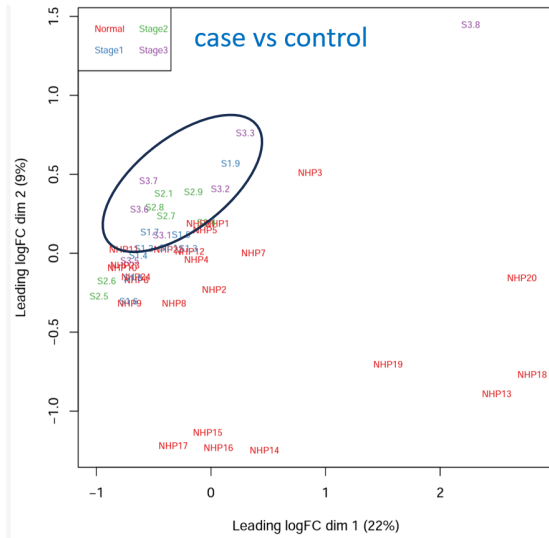
INOVIQ EXO-NET® **+ Promega** Maxwell® HT miRNA Plasma and Serum kit enables EV cargo analysis

Top GO Pathway Analysis Between Stage 3&4 vs Normal

Cellular Component

Biological Process

Molecular Function

INOVIQ

miRNA Net
Healthy vs Stage III Ovarian Cancer

Feature selection
adjusted p value = 0.05
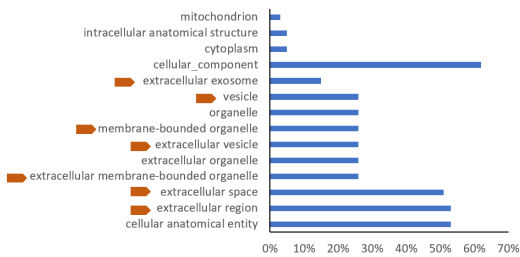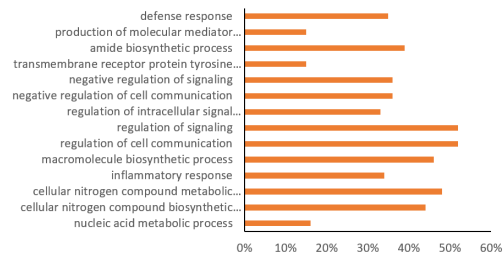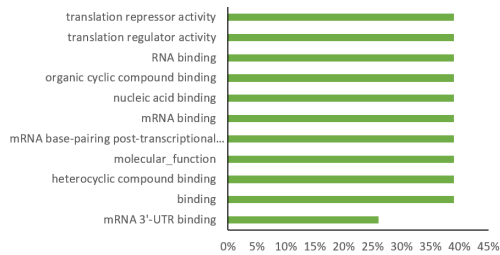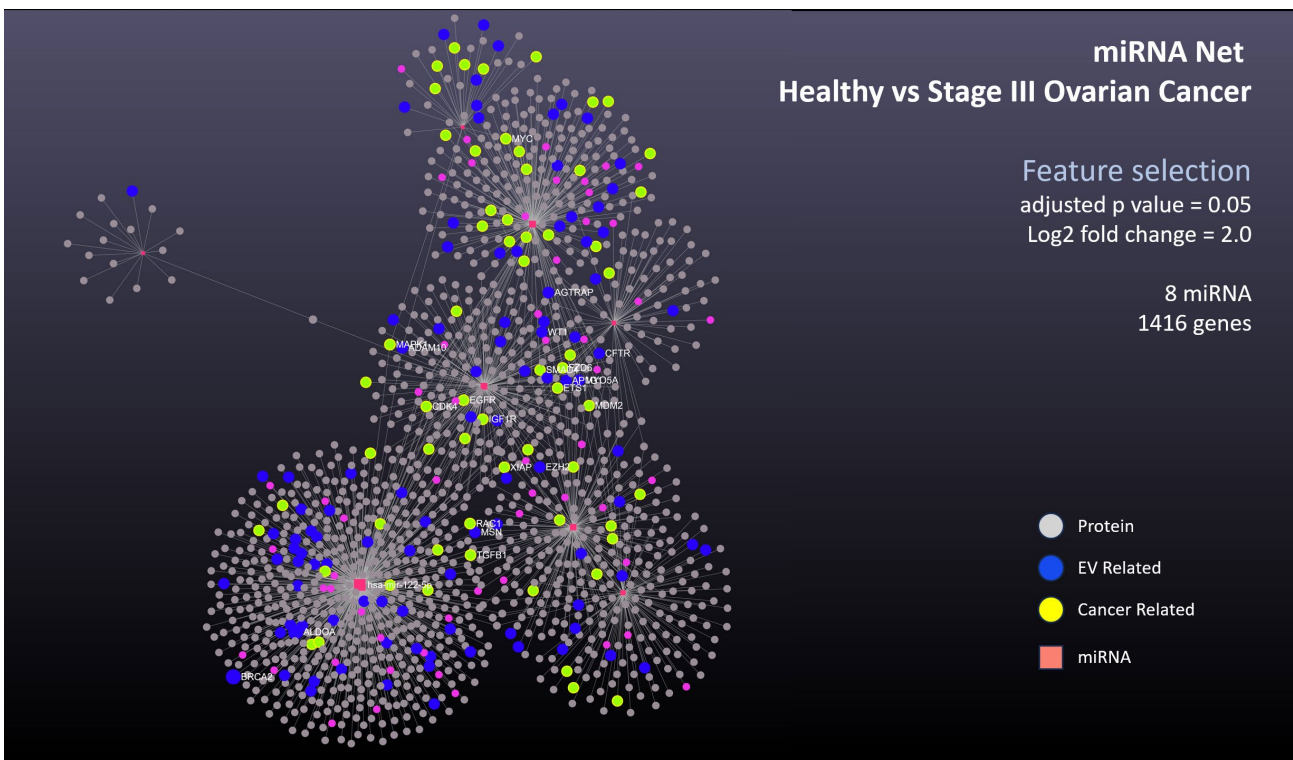Log2 fold change = 2.0

8 miRNA
1416 genes

○ Protein
● EV Related
● Cancer Related
■ miRNA

Outcome: miRNA obtained using EXO-NET® and Maxwell® HT miRNA Plasma and Serum Kit on a high-throughput, fully automated platform was fit-for-purpose for miRNASeq.

Identifying 27 significantly differentially expressed miRNAs (log2 =2, p <0.05) from a subpopulation of plasma EVs obtain from normal healthy women and women diagnosed with ovarian cancer.

Data modelling identified molecular pathways associated with ovarian cancer and EV compartments.

5.4 MIRNASEQ ANALYSIS OF EXO-NET ISOLATED PLASMA EVS

5.4.1 Ovarian Cancer

Aim: Identify differential expression of targeted exosomal miRNAs in a subpopulation of EVs isolated from plasma samples obtain from normal healthy women and women diagnosed with ovarian cancer.

Intended Use: For research of treatment response monitoring, disease recurrence.

Project Plan:

Ovarian Cancer | HT Isolation of EVS and Targeted MicroRNA Screening

Serum (0.5ml): ovarian cancer (I,II,III, n=26) and control (n=24)

10,000g for 5 min

Automated isolation of EVs (EXO-NET®) and RNA (Promega Maxwell® HT miRNA Plasma and Serum isolation kit) Kingfisher Apex

Bioanalyzer RNA QC

TaqMan™ Advanced miRNA cDNA Synthesis Kit

QuantStudio Real-Time PCR
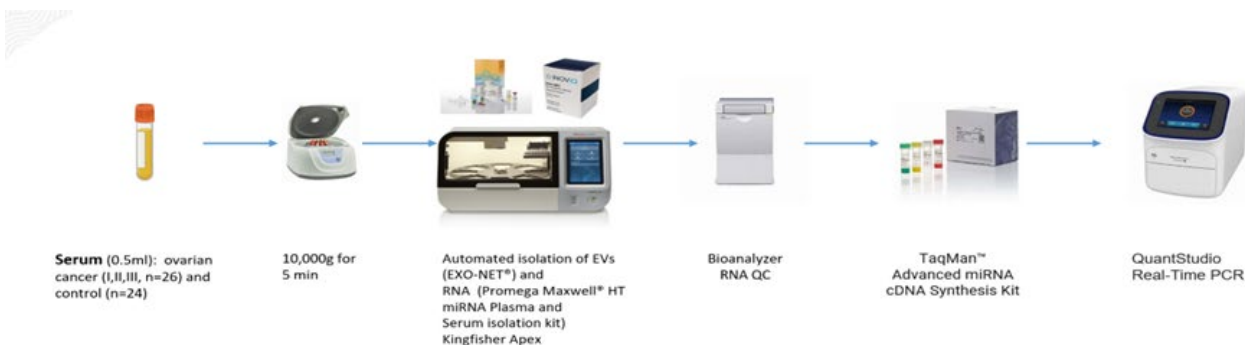
qPCR of 16 targeted miRNAs
24 controls, 9 stage I, 9 stage II and 8 stage III

INOVIQ

Results:

RT-qPCR Analysis of Targeted microRNAs
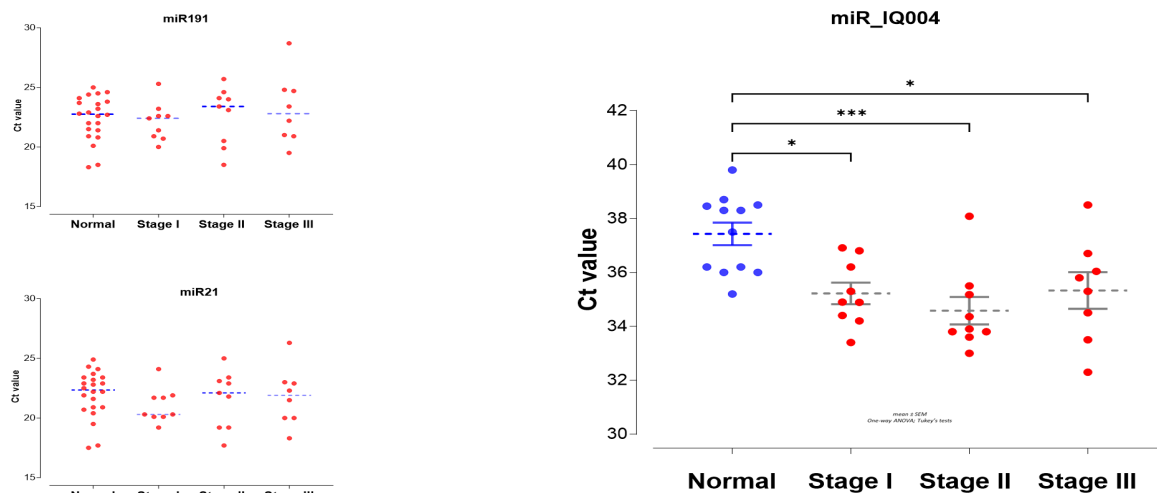
Outcome: miRNA obtained using EXO-NET® and Maxwell® HT miRNA Plasma and Serum kit on a high-throughput, fully automated platform was fit-for-purpose for RT qPCR analysis. All 16 miRNA were present in control and case plasma samples. 3 miRNA were consistently expressed in all samples. One miRNA miRNA_IQ004 was significantly differentially expressed at all stages of ovarian cancer compared to controls.

5.5 DESIGN OUTPUTS

INPUT	SPECIFICATION	OUTPUT
Rapid	<2min avg per sample	1.25 min/sample
High throughput	400 samples per day	384 - 4 plates
Cost effective	Price competitive	Comparable
Reproducible	Endpoint measure intra run CV <10% inter run CV <20%	Achieved (total RNA/Protein)
Low sample volume	500 µl plasma 1 ml CCM	200 µl plasma 1 ml CCM
Total protein yield	< 10 µg/sample	10-12 µg/sample
Total RNA yield	< 3 ng/sample	3-5 ng/sample
Scalability	Manual & full automation	Full automation achieved
Compatibility	Isolates compatible with commercially available kits	Developed using Promega kits

INOVIQ

6. REFERENCES

[1] C. Salomon, S. Das, U. Erdbrugger, R. Kalluri, S. Kiang Lim, J.M. Olefsky, G.E. Rice, S. Sahoo, W. Andy Tao, P. Vader, Q. Wang, A.M. Weaver, Extracellular Vesicles and Their Emerging Roles as Cellular Messengers in Endocrinology: An Endocrine Society Scientific Statement, Endocr Rev (2022).

[2] F. Puhm, L. Flamand, E. Boilard, Platelet extracellular vesicles in COVID-19: Potential markers and makers, J Leukoc Biol 111(1) (2022) 63-74.

[3] J. Penders, A. Nagelkerke, E.M. Cunnane, S.V. Pedersen, I.J. Pence, R.C. Coombes, M.M. Stevens, Single Particle Automated Raman Trapping Analysis of Breast Cancer Cell-Derived Extracellular Vesicles as Cancer Biomarkers, ACS Nano (2021).

[4] Y. Yi, M. Wu, H. Zeng, W. Hu, C. Zhao, M. Xiong, W. Lv, P. Deng, Q. Zhang, Y. Wu, Tumor-Derived Exosomal Non-Coding RNAs: The Emerging Mechanisms and Potential Clinical Applications in Breast Cancer, Front Oncol 11 (2021) 738945.

[5] S.R. Douglas, K.T. Yeung, J. Yang, S.L. Blair, O. Cohen, B.P. Eliceiri, Identification of CD105+ Extracellular Vesicles as a Candidate Biomarker for Metastatic Breast Cancer, J Surg Res 268 (2021) 168-173.

[6] H. Su, Y.H. Rustam, C.L. Masters, E. Makalic, C.A. McLean, A.F. Hill, K.J. Barnham, G.E. Reid, L.J. Vella, Characterization of brain-derived extracellular vesicle lipids in Alzheimer's disease, J Extracell Vesicles 10(7) (2021) e12089.

[7] T. Kato, J.V. Vykoukal, J.F. Fahrmann, S. Hanash, Extracellular Vesicles in Lung Cancer: Prospects for Diagnostic and Therapeutic Applications, Cancers (Basel) 13(18) (2021).

[8] M. Surman, S. Kedracka-Krok, D. Hoja-Lukowicz, U. Jankowska, A. Drozdz, E.L. Stepien, M. Przybylo, Mass Spectrometry-Based Proteomic Characterization of Cutaneous Melanoma Ectosomes Reveals the Presence of Cancer-Related Molecules, Int J Mol Sci 21(8) (2020).

[9] A. Nanou, L.L. Zeune, F.C. Bidard, J.Y. Pierga, L. Terstappen, HER2 expression on tumor-derived extracellular vesicles and circulating tumor cells in metastatic breast cancer, Breast Cancer Res 22(1) (2020) 86.

[10] S. Kim, M.C. Choi, J.Y. Jeong, S. Hwang, S.G. Jung, W.D. Joo, H. Park, S.H. Song, C. Lee, T.H. Kim, H.J. An, Serum exosomal miRNA-145 and miRNA-200c as promising biomarkers for preoperative diagnosis of ovarian carcinomas, J Cancer 10(9) (2019) 1958-1967.

[11] R. Tutrone, M.J. Donovan, P. Torkler, V. Tadigotla, T. McLain, M. Noerholm, J. Skog, J. McKiernan, Clinical utility of the exosome based ExoDx Prostate(IntelliScore) EPI test in men presenting for initial Biopsy with a PSA 2-10 ng/mL, Prostate Cancer Prostatic Dis 23(4) (2020) 607-614.

[12] N. Arraud, R. Linares, S. Tan, C. Gounou, J.M. Pasquet, S. Mornet, A.R. Brisson, Extracellular vesicles from blood plasma: determination of their morphology, size, phenotype and concentration, J Thromb Haemost 12(5) (2014) 614-27.

[13] J.R. Edgar, E.R. Eden, C.E. Futter, Hrs- and CD63-dependent competing mechanisms make different sized endosomal intraluminal vesicles, Traffic 15(2) (2014) 197-211.

[14] G. van Niel, G. D'Angelo, G. Raposo, Shedding light on the cell biology of extracellular vesicles, Nat Rev Mol Cell Biol 19(4) (2018) 213-228.

[15] J. Meldolesi, Exosomes and Ectosomes in Intercellular Communication, Curr Biol 28(8) (2018) R435-R444.

[16] T.K. Phan, D.C. Ozkocak, I.K.H. Poon, Unleashing the therapeutic potential of apoptotic bodies, Biochem Soc Trans 48(5) (2020) 2079-2088.

[17] R.M. Johnstone, M. Adam, J. Hammond, L. Orr, C. Turbide, Vesicle formation during reticulocyte maturation. Association of plasma membrane activities with released vesicles (exosomes), Journal of Biological Chemistry 262(19) (1987) 9412-9420.

[18] J. Kowal, M. Tkach, C. Théry, Biogenesis and secretion of exosomes, Curr Opin Cell Biol 29 (2014) 116-25.

[19] R.A. Dragovic, C. Gardiner, A.S. Brooks, D.S. Tannetta, D.J. Ferguson, P. Hole, B. Carr, C.W. Redman, A.L. Harris, P.J. Dobson, P. Harrison, I.L. Sargent, Sizing and phenotyping of cellular vesicles using Nanoparticle Tracking Analysis, Nanomedicine 7 (2011).

INOVIQ

[20] E.J. van der Vlist, E.N. Nolte-'t Hoen, W. Stoorvogel, G.J. Arkesteijn, M.H. Wauben, Fluorescent labeling of nano-sized vesicles released by cells and subsequent quantitative and qualitative analysis by high-resolution flow cytometry, Nat Protoc 7(7) (2012) 1311-26.

[21] J. Kowal, G. Arras, M. Colombo, M. Jouve, J.P. Morath, B. Primdal-Bengtson, F. Dingli, D. Loew, M. Tkach, C.J.P.o.t.N.A.o.S. Théry, Proteomic comparison defines novel markers to characterize heterogeneous populations of extracellular vesicle subtypes, Proc Natl Acad Sci U S A 113(8) (2016) E968-E977.

[22] C. Théry, K.W. Witwer, E. Aikawa, M.J. Alcaraz, J.D. Anderson, R. Andriantsitohaina, A. Antoniou, T. Arab, F. Archer, G.K. Atkin-Smith, D.C. Ayre, J.-M. Bach, D. Bachurski, H. Baharvand, L. Balaj, S. Baldacchino, N.N. Bauer, A.A. Baxter, M. Bebawy, C. Beckham, A. Bedina Zavec, A. Benmoussa, A.C. Berardi, P. Bergese, E. Bielska, C. Blenkiron, S. Bobis-Wozowicz, E. Boilard, W. Boireau, A. Bongiovanni, F.E. Borràs, S. Bosch, C.M. Boulanger, X. Breakefield, A.M. Breglio, M.Á. Brennan, D.R. Brigstock, A. Brisson, M.L. Broekman, J.F. Bromberg, P. Bryl-Górecka, S. Buch, A.H. Buck, D. Burger, S. Busatto, D. Buschmann, B. Bussolati, E.I. Buzás, J.B. Byrd, G. Camussi, D.R. Carter, S. Caruso, L.W. Chamley, Y.-T. Chang, C. Chen, S. Chen, L. Cheng, A.R. Chin, A. Clayton, S.P. Clerici, A. Cocks, E. Cocucci, R.J. Coffey, A. Cordeiro-da-Silva, Y. Couch, F.A. Coumans, B. Coyle, R. Crescitelli, M.F. Criado, C. D'Souza-Schorey, S. Das, A. Datta Chaudhuri, P. de Candia, E.F. De Santana, O. De Wever, H.A. Del Portillo, T. Demaret, S. Deville, A. Devitt, B. Dhondt, D. Di Vizio, L.C. Dieterich, V. Dolo, A.P. Dominguez Rubio, M. Dominici, M.R. Dourado, T.A. Driedonks, F.V. Duarte, H.M. Duncan, R.M. Eichenberger, K. Ekström, S. El Andaloussi, C. Elie-Caille, U. Erdbrügger, J.M. Falcón-Pérez, F. Fatima, J.E. Fish, M. Flores-Bellver, A. Försönits, A. Frelet-Barrand, F. Fricke, G. Fuhrmann, S. Gabrielsson, A. Gámez-Valero, C. Gardiner, K. Gärtner, R. Gaudin, Y.S. Gho, B. Giebel, C. Gilbert, M. Gimona, I. Giusti, D.C. Goberdhan, A. Görgens, S.M. Gorski, D.W. Greening, J.C. Gross, A. Gualerzi, G.N. Gupta, D. Gustafson, A. Handberg, R.A. Haraszti, P. Harrison, H. Hegyesi, A. Hendrix, A.F. Hill, F.H. Hochberg, K.F. Hoffmann, B. Holder, H. Holthofer, B. Hosseinkhani, G. Hu, Y. Huang, V. Huber, S. Hunt, A.G.-E. Ibrahim, T. Ikezu, J.M. Inal, M. Isin, A. Ivanova, H.K. Jackson, S. Jacobsen, S.M. Jay, M. Jayachandran, G. Jenster, L. Jiang, S.M. Johnson, J.C. Jones, A. Jong, T. Jovanovic-Talisman, S. Jung, R. Kalluri, S.-I. Kano, S. Kaur, Y. Kawamura, E.T. Keller, D. Khamari, E. Khomyakova, A. Khvorova, P. Kierulf, K.P. Kim, T. Kislinger, M. Klingeborn, D.J. Klinke, 2nd, M. Kornek, M.M. Kosanović, Á.F. Kovács, E.-M. Krämer-Albers, S. Krasemann, M. Krause, I.V. Kurochkin, G.D. Kusuma, S. Kuypers, S. Laitinen, S.M. Langevin, L.R. Languino, J. Lannigan, C. Lässer, L.C. Laurent, G. Lavieu, E. Lázaro-Ibáñez, S. Le Lay, M.-S. Lee, Y.X.F. Lee, D.S. Lemos, M. Lenassi, A. Leszczynska, I.T. Li, K. Liao, S.F. Libregts, E. Ligeti, R. Lim, S.K. Lim, A. Linē, K. Linnemannstöns, A. Llorente, C.A. Lombard, M.J. Lorenowicz, Á.M. Lörincz, J. Lötvall, J. Lovett, M.C. Lowry, X. Loyer, Q. Lu, B. Lukomska, T.R. Lunavat, S.L. Maas, H. Malhi, A. Marcilla, J. Mariani, J. Mariscal, E.S. Martens-Uzunova, L. Martin-Jaular, M.C. Martinez, V.R. Martins, M. Mathieu, S. Mathivanan, M. Maugeri, L.K. McGinnis, M.J. McVey, D.G. Meckes, Jr., K.L. Meehan, I. Mertens, V.R. Minciacchi, A. Möller, M. Møller Jørgensen, A. Morales-Kastresana, J. Morhayim, F. Mullier, M. Muraca, L. Musante, V. Mussack, D.C. Muth, K.H. Myburgh, T. Najrana, M. Nawaz, I. Nazarenko, P. Nejsum, C. Neri, T. Neri, R. Nieuwland, L. Nimrichter, J.P. Nolan, E.N. Nolte-'t Hoen, N. Noren Hooten, L. O'Driscoll, T. O'Grady, A. O'Loghlen, T. Ochiya, M. Olivier, A. Ortiz, L.A. Ortiz, X. Osteikoetxea, O. Østergaard, M. Ostrowski, J. Park, D.M. Pegtel, H. Peinado, F. Perut, M.W. Pfaffl, D.G. Phinney, B.C. Pieters, R.C. Pink, D.S. Pisetsky, E. Pogge von Strandmann, I. Polakovicova, I.K. Poon, B.H. Powell, I. Prada, L. Pulliam, P. Quesenberry, A. Radeghieri, R.L. Raffai, S. Raimondo, J. Rak, M.I. Ramirez, G. Raposo, M.S. Rayyan, N. Regev-Rudzki, F.L. Ricklefs, P.D. Robbins, D.D. Roberts, S.C. Rodrigues, E. Rohde, S. Rome, K.M. Rouschop, A. Rughetti, A.E. Russell, P. Saá, S. Sahoo, E. Salas-Huenuleo, C. Sánchez, J.A. Saugstad, M.J. Saul, R.M. Schiffelers, R. Schneider, T.H. Schøyen, A. Scott, E. Shahaj, S. Sharma, O. Shatnyeva, F. Shekari, G.V. Shelke, A.K. Shetty, K. Shiba, P.R.M. Siljander, A.M. Silva, A. Skowronek, O.L. Snyder, 2nd, R.P. Soares, B.W. Sódar, C. Soekmadji, J. Sotillo, P.D. Stahl, W. Stoorvogel, S.L. Stott, E.F. Strasser, S. Swift, H. Tahara, M. Tewari, K. Timms, S. Tiwari, R. Tixeira, M. Tkach, W.S. Toh, R. Tomasini, A.C. Torrecilhas, J.P. Tosar, V. Toxavidis, L. Urbanelli, P. Vader, B.W. van Balkom, S.G. van der Grein, J. Van Deun, M.J. van Herwijnen, K. Van Keuren-Jensen, G. van Niel, M.E. van Royen, A.J. van Wijnen, M.H. Vasconcelos, I.J. Vechetti, Jr., T.D. Veit, L.J. Vella, É. Velot, F.J. Verweij, B. Vestad, J.L. Viñas, T. Visnovitz, K.V. Vukman, J. Wahlgren, D.C. Watson, M.H. Wauben, A. Weaver, J.P. Webber, V. Weber, A.M. Wehman, D.J. Weiss, J.A. Welsh, S. Wendt, A.M. Wheelock, Z. Wiener, L. Witte, J. Wolfram, A. Xagorari, P. Xander, J. Xu, X. Yan, M. Yáñez-Mó, H. Yin, Y. Yuana, V. Zappulli, J. Zarubova, V. Žèkas, J.-Y. Zhang, Z. Zhao, L. Zheng, A.R. Zheutlin, A.M. Zickler, P. Zimmermann, A.M. Zivkovic, D. Zocco, E.K. Zuba-Surma, Minimal information for studies of extracellular vesicles 2018 (MISEV2018): a position statement of the International Society for Extracellular Vesicles and update of the MISEV2014 guidelines, Journal of extracellular vesicles 7(1) (2018) 1535750-1535750.

INOVIQ

[23] D.K. Jeppesen, A.M. Fenix, J.L. Franklin, J.N. Higginbotham, Q. Zhang, L.J. Zimmerman, D.C. Liebler, J. Ping, Q. Liu, R. Evans, Reassessment of exosome composition, Cell 177(2) (2019) 428-445. e18.

[24] M. Yáñez-Mó, P.R.M. Siljander, Z. Andreu, A. Bedina Zavec, F.E. Borràs, E.I. Buzas, K. Buzas, E. Casal, F. Cappello, J. Carvalho, E. Colás, A. Cordeiro-da Silva, S. Fais, J.M. Falcon-Perez, I.M. Ghobrial, B. Giebel, M. Gimona, M. Graner, I. Gursel, M. Gursel, N.H.H. Heegaard, A. Hendrix, P. Kierulf, K. Kokubun, M. Kosanovic, V. Kralj-Iglic, E.-M. Krämer-Albers, S. Laitinen, C. Lässer, T. Lener, E. Ligeti, A. Linē, G. Lipps, A. Llorente, J. Lötvall, M. Manček-Keber, A. Marcilla, M. Mittelbrunn, I. Nazarenko, E.N.M. Nolte-'t Hoen, T.A. Nyman, L. O'Driscoll, M. Olivan, C. Oliveira, É. Pállinger, H.A. del Portillo, J. Reventós, M. Rigau, E. Rohde, M. Sammar, F. Sánchez-Madrid, N. Santarém, K. Schallmoser, M. Stampe Ostenfeld, W. Stoorvogel, R. Stukelj, S.G. Van der Grein, M. Helena Vasconcelos, M.H.M. Wauben, O. De Wever, Biological properties of extracellular vesicles and their physiological functions, Journal of Extracellular Vesicles 4(1) (2015) 27066.

[25] R.A. Dragovic, J.H. Southcombe, D.S. Tannetta, C.W. Redman, I.L. Sargent, Multicolor flow cytometry and nanoparticle tracking analysis of extracellular vesicles in the plasma of normal pregnant and pre-eclamptic women, Biol Reprod 89(6) (2013) 151.

[26] N. Arraud, R. Linares, S. Tan, C. Gounou, J.M. Pasquet, S. Mornet, A.R. Brisson, Extracellular vesicles from blood plasma: determination of their morphology, size, phenotype and concentration, Journal of Thrombosis and Haemostasis 12(5) (2014) 614-627.

[27] B. da Rocha-Azevedo, S.L. Schmid, Migrasomes: a new organelle of migrating cells, Cell Research 25(1) (2015) 1-2.

[28] S. Tavano, C.-P. Heisenberg, Migrasomes take center stage, Nature Cell Biology 21(8) (2019) 918-920.

[29] L. Ma, Y. Li, J. Peng, D. Wu, X. Zhao, Y. Cui, L. Chen, X. Yan, Y. Du, L. Yu, Discovery of the migrasome, an organelle mediating release of cytoplasmic contents during cell migration, Cell Res 25(1) (2015) 24-38.

[30] S. Caruso, I.K.H. Poon, Apoptotic Cell-Derived Extracellular Vesicles: More Than Just Debris, Frontiers in immunology 9 (2018) 1486-1486.

[31] J. Suzuki, D.P. Denning, E. Imanishi, H.R. Horvitz, S. Nagata, Xk-related protein 8 and CED-8 promote phosphatidylserine exposure in apoptotic cells, Science 341(6144) (2013) 403-6.

[32] V.R. Minciacchi, S. You, C. Spinelli, S. Morley, M. Zandian, P.J. Aspuria, L. Cavallini, C. Ciardiello, M. Reis Sobreiro, M. Morello, G. Kharmate, S.C. Jang, D.K. Kim, E. Hosseini-Beheshti, E. Tomlinson Guns, M. Gleave, Y.S. Gho, S. Mathivanan, W. Yang, M.R. Freeman, D. Di Vizio, Large oncosomes contain distinct protein cargo and represent a separate functional class of tumor-derived extracellular vesicles, Oncotarget 6(13) (2015) 11327-41.

[33] K. Al-Nedawi, B. Meehan, J. Micallef, V. Lhotak, L. May, A. Guha, J. Rak, Intercellular transfer of the oncogenic receptor EGFRvIII by microvesicles derived from tumour cells, Nat Cell Biol 10(5) (2008) 619-24.

[34] D. Di Vizio, J. Kim, M.H. Hager, M. Morello, W. Yang, C.J. Lafargue, L.D. True, M.A. Rubin, R.M. Adam, R. Beroukhim, F. Demichelis, M.R. Freeman, Oncosome Formation in Prostate Cancer: Association with a Region of Frequent Chromosomal Deletion in Metastatic Disease, Cancer Research 69(13) (2009) 5601-5609.

[35] J.F. Nabhan, R. Hu, R.S. Oh, S.N. Cohen, Q. Lu, Formation and release of arrestin domain-containing protein 1-mediated microvesicles (ARMMs) at plasma membrane by recruitment of TSG101 protein, Proc Natl Acad Sci U S A 109(11) (2012) 4146-51.

[36] Q. Wang, Q. Lu, Plasma membrane-derived extracellular microvesicles mediate non-canonical intercellular NOTCH signaling, Nat Commun 8(1) (2017) 709.

[37] D. Perez-Hernandez, C. Gutierrez-Vazquez, I. Jorge, S. Lopez-Martin, A. Ursa, F. Sanchez-Madrid, J. Vazquez, M. Yanez-Mo, The intracellular interactome of tetraspanin-enriched microdomains reveals their function as sorting machineries toward exosomes, J Biol Chem 288(17) (2013) 11649-61.

[38] S.J. Israels, E.M. McMillan-Ward, J. Easton, C. Robertson, A. McNicol, CD63 associates with the alphaIIb beta3 integrin-CD9 complex on the surface of activated platelets, Thromb Haemost 85(1) (2001) 134-41.

[39] M.E. Hemler, Tetraspanin functions and associated microdomains, Nat Rev Mol Cell Biol 6(10) (2005) 801-11.

INOVIQ

[40] R.C. Lai, F. Arslan, M.M. Lee, N.S. Sze, A. Choo, T.S. Chen, M. Salto-Tellez, L. Timmers, C.N. Lee, R.M. El Oakley, G. Pasterkamp, D.P. de Kleijn, S.K. Lim, Exosome secreted by MSC reduces myocardial ischemia/reperfusion injury, Stem Cell Res 4(3) (2010) 214-22.

[41] N. Sumiyoshi, H. Ishitobi, S. Miyaki, K. Miyado, N. Adachi, M. Ochi, The role of tetraspanin CD9 in osteoarthritis using three different mouse models, Biomed Res 37(5) (2016) 283-291.

INOV**IQ**